APOLLO SPACECRAFT

FINAL REPORT

ASPO TASK 18
LEM AND CSM USB SYSTEM RF TRACKING STUDY

2231-6006-T0-000   January 1966

Prepared for
NASA MANNED SPACECRAFT CENTER
Houston, Texas
Under
Contract No. NAS9-4810

TRW SYSTEMS
One Space Park · Redondo Beach, California

Prepared _____
             T. C. Larter

Prepared _____
             K. E. Lytal

Approved _____
             G. S. Kasai
             Manager
             Antenna Systems Department

Approved _____
             H. T. Hayes
             Manager
             Communication Laboratory

CONTENTS

ILLUSTRATIONS

ILLUSTRATIONS (Continued)

1. INTRODUCTION AND SUMMARY

The purpose of the RF tracking task is to investigate the interface compatibility of the RF tracking concept and the operation of the Unified S-Band System. The RF tracking concept proposed for the Apollo LEM and CSM high gain antennas introduces phase and amplitude modulation on the USBS uplink carrier at the switching frequency. The switching function is required to generate an error signal with a minimum of additional equipment. The ultimate objective of this task is to determine the effects of the RF tracking on the performance of the Unified S-Band System.

The analysis first considers the similarity of pure amplitude and pure phase comparison antennas for generating a steering error signal. It is then pointed out that any real antenna system contains both amplitude and phase comparison components which produce PM and AM in the output signal. An equation is developed which relates the vector output voltage relationships to the physical parameters of the antenna system.

The analysis is based on a pure linear polarized wave which is aligned with linear polarized elements in the antenna. The results would also be correct for circular polarization where the antenna elements and the received wave have the same direction of rotation and are purely circular. The case of elliptical polarization and antennas with axial ratios which differ from 1.0 is not considered because information was not available on the orientation of the elliptical axes. The CSM antennas have identical circularly polarized elements which tend to minimize the elliptical polarization problem. The LEM, on the other hand, has a circularly polarized antenna for the sum signal and linearly polarized slots for the difference signal.

Computer solutions were obtained for the LEM and CSM antennas based on the data obtained from the LEM Design Review No. 1 and the "CSM 60 Day Study Final Report" from the Dalmo-Victor Co.

Variations in squint angle, coupling factor, and phase error ahead of the sum and difference network were also run on the computer to show their effect on modulation.

Computer results using the most likely values for each of the physical parameters are summarized in the table below:

	Acquisition Range	Phase Modulation Sensitivity PM^{o}/Steering Angle
CSM Wide Mode	$\pm 38^{o}$	0.1^{o}/Degree
CMS Narrow Mode	$\pm 4.7^{o}$	0.5^{o}/Degree
LEM	-12° to $+16^{o}$	0.5^{o}/Degree

The effects of RF tracking on the Unified S-Band Communication System are analyzed. It is concluded that with the values of null depth, coupling factors, and squint angle used in the LEM and CSM RF trackers, the effects on the ranging and communication channels will be negligible During acquisition, it may be possible for the transponder carrier tracking loop to lock on a sideband produced by incidental phase modulation. This is unlikely, but if considered a serious defect, the problem can be completely eliminated by suspending lobing during acquisition.

Acquisition time will be increased from previous estimates by the slewing time of the antenna under worst case conditions.

2. ANALYSIS OF TRACKING ANTENNA PATTERNS

The principle behind automatic tracking antennas is the comparison of the received signal on two separate antennas. If amplitude comparison is to be made, the two antennas are mounted as close together as possible and their beams squinted the same angle "α" on either side of boresight as shown in Figure 1. For phase comparison, the beams are pointed in the same direction and the antennas separated a distance "s" from the axis to obtain an interferometer effect.

If the amplitude comparison (A. C.) were made without any phase error or the phase comparison (P. C.) mode were at exactly the same amplitude from each antenna, the output could be made to produce pure AM without PM. Figure 2 shows vector relationships for a typical case a little off boresight. It should be noted that by rotating the Δ vector $90°$ either antenna system can be made equivalent to the other at the output of the Σ and Δ network.[1]

In either case mechanical and electrical imperfections are always present which result in amplitude and phase errors.

The output voltage and phase from each antenna can be related to the physical parameters and steering error angle θ by equations which are the same for either system.

$$E_1 = A_1 \frac{\sin k(\theta - \alpha)}{k(\theta - \alpha)} e^{-i\varphi}$$

$$E_2 = A_2 \frac{\sin k(\theta + \alpha)}{k(\theta + \alpha)} e^{i(\varphi + \delta)}$$

A = amplitude factor
k = angular scale factor
θ = steering error angle
α = squint angle

[1] Rhodes, D. R., "Introduction to Monopulse," McGraw-Hill, 1959, p. 29.
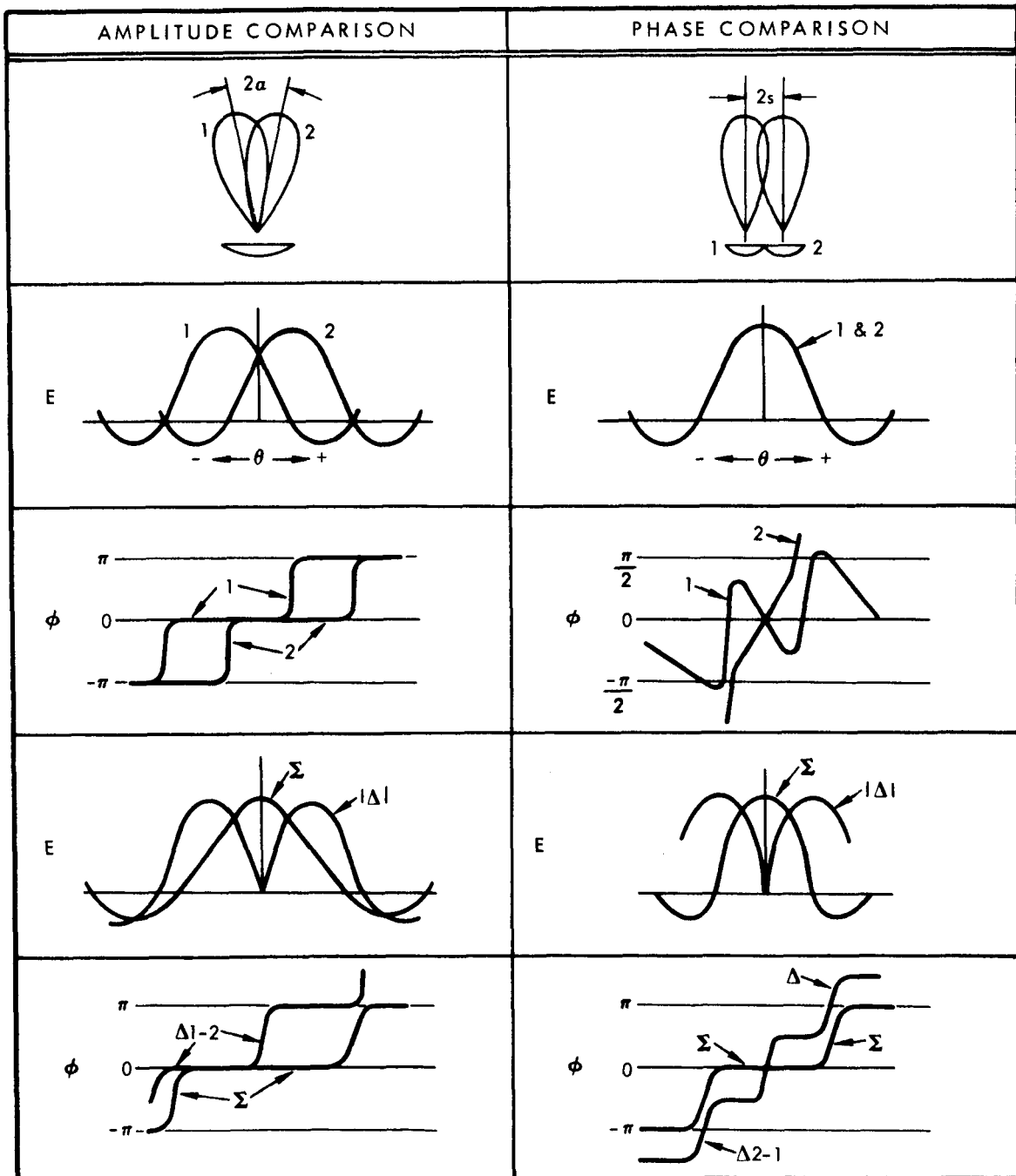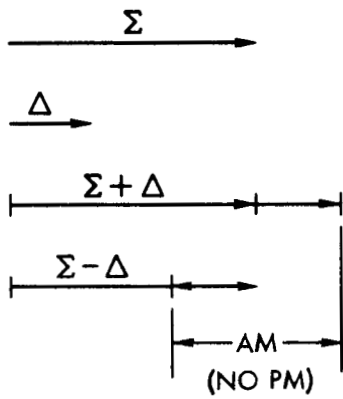
Figure 1. Amplitude and Phase Comparison Antennas
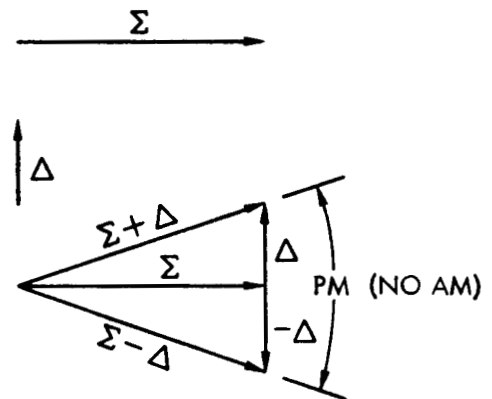
AMPLITUDE COMPARISON

PHASE COMPARISON

Figure 2.   Vector Addition Off Boresight

$$\varphi = \text{phase function} = \frac{2\pi s}{\lambda} \sin \theta$$

s = spacing of phase center from boresight axis

λ = wavelength

δ = phase error before comparator

The value of each term in the equations can be determined from either physical parameters of the antenna or examination of the antenna patterns. The most common antenna patterns for tracking antennas are the "sum" and "difference" patterns. They are obtained from the elemental patterns by

$$E_\Sigma = E_1 + E_2$$

$$E_\Delta = E_1 - E_2$$

The angular scale factor is used to match the $\sin x / x$ function to the actual pattern. A good method is to make the value of $k\theta$ at the 3 db points of the pattern of a single element equal to 1.39. This value produces 0.707 from $\sin k\theta / k\theta$.[2]

The depth and position of the difference pattern null establishes several more parameters for the equations. The depth of the null is primarily a function of the pre-comparator phase error "δ" in an A.C. system, or in a P.C. system, a function of the amplitude ratio A_1/A_2.[3] Position of the null, or boresight shift, depends on the reverse-amplitude ratio in an A.C. system and phase error in a P.C. system. Null depths are measured relative to the peak of the sum pattern, and boresight shift is measured relative to the mechanical boresight.

---

[2] Jahnke and Emde, Tables of Functions, Fourth Edition Addenda, p. 33.

[3] Cohen and Steinmetz, "Amplitude and Phase Sensing Monopulse System Parameters," Microwave Journal, October and November 1959.

For an A. C. system

$$\frac{E_{\Delta_n}}{E_{\Sigma_\rho}} = \frac{1-e^{i\delta}}{2\cos\alpha}$$

For a P. C. system

$$\frac{E_{\Delta_n}}{E_{\Sigma_\rho}} = \frac{A_1}{2A_2}$$

These quantities are plotted in Figures 3 and 4.

Boresight shift in a P. C. system is equal to $\delta/2$ for small values of δ. In an A. C. system the shift is related to the squint angle and amplitude ratio which can be found by equating the individual pattern equation at θ_s

$$A_1 \frac{\sin(\theta_s - \alpha)}{\theta_s - \alpha} = A_2 \frac{\sin(\theta_s + \alpha)}{\theta_s + \alpha}$$

$$\frac{A_1}{A_2} = \frac{\sin\theta_s + \alpha}{\theta_s + \alpha} \cdot \frac{\theta_s - \alpha}{\sin(\theta_s - \alpha)}$$

for $\theta_s < \dfrac{\pi}{20}$, $\alpha < \dfrac{\pi}{10}$

$$\cong \frac{\cos(\theta_s + \alpha)}{\cos(\theta_s - \alpha)}$$

$$= \frac{\cos\theta_s \cos\alpha - \sin\theta_s \sin\alpha}{\cos\theta_s \cos\alpha + \sin\theta_s \sin\alpha}$$

$$\cong \frac{\cos\alpha - \theta_s \sin\alpha}{\cos\alpha + \theta_s \sin\alpha} = \frac{1 - \theta_s \tan\alpha}{1 + \theta_s \tan\alpha}$$
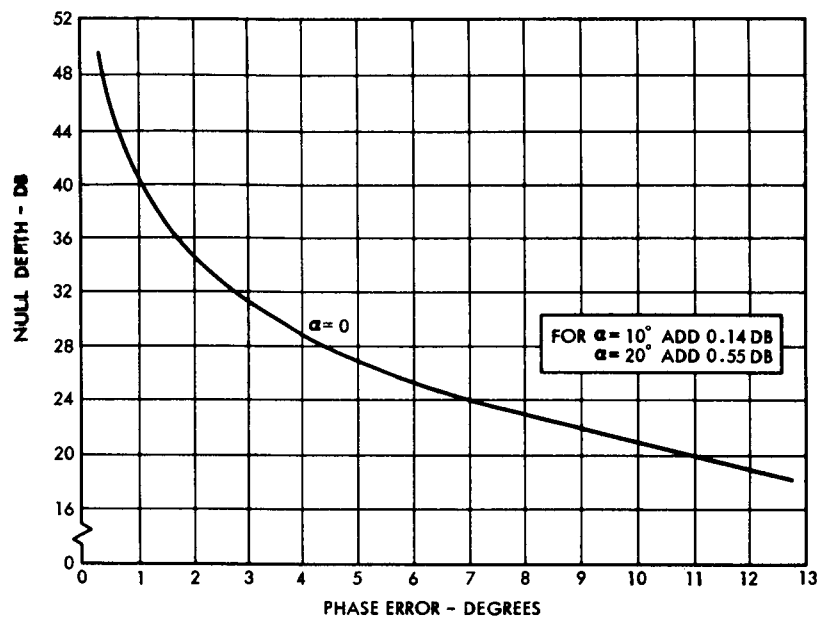
Figure 3. Null Depth vs Phase Error
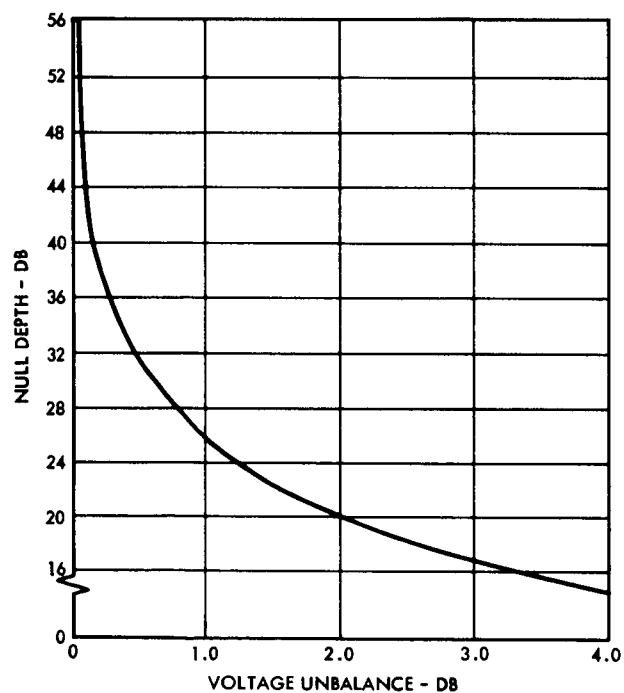for Amplitude Comparison System

Figure 4. Null Depth vs Voltage Unbalance
for Phase Comparison System

$$\theta_s = \cot \alpha \, \frac{1 - A_1/A_2}{1 - A_1/A_2}$$

This function is plotted in Figure 5 over a range to 2 db unbalance and $16°$ of squint angle.

The point where E_Σ and E_Δ on the antenna patterns can be used to determine the value of ϕ for phase comparison systems and also amplitude systems if s has an appreciable value. When two vectors are added and subtracted and result in the same absolute value, they must be in quadrature regardless of their individual values. In the case of a phase comparison system, the individual values are nearly equal while in an amplitude system one of them is almost zero. It is impossible to place the phase centers of the two separate antennas in an amplitude comparison system at the same point; therefore, the separation distance between them gives rise to a phase factor which determines the location of the E_Σ and E_Δ point if α is greater than the beamwidth. In either system δ is found first, then ϕ determined from $2\phi + \delta = 90°$. In an amplitude system, δ is found from the difference pattern null as explained above and in a phase system δ is equal to twice the value of boresight shift.

The equation for phase center spacing is

$$s/\lambda = \frac{90° - \delta}{720° \sin \theta_{\Sigma = \Delta}}$$

Figure 6 shows this function plotted for $\delta = 1°$ and $8°$ over a range of $\theta_{\Sigma = \Delta}$ from 0 to $28°$ and 2s up to 15 wavelengths.

Squint angle can be related to the ratio of sum signal level at $\theta = 0$ to the level at $E_\Sigma = E_\Delta$; however, this calculation requires very accurate angle and level measurements. If the physical dimensions of
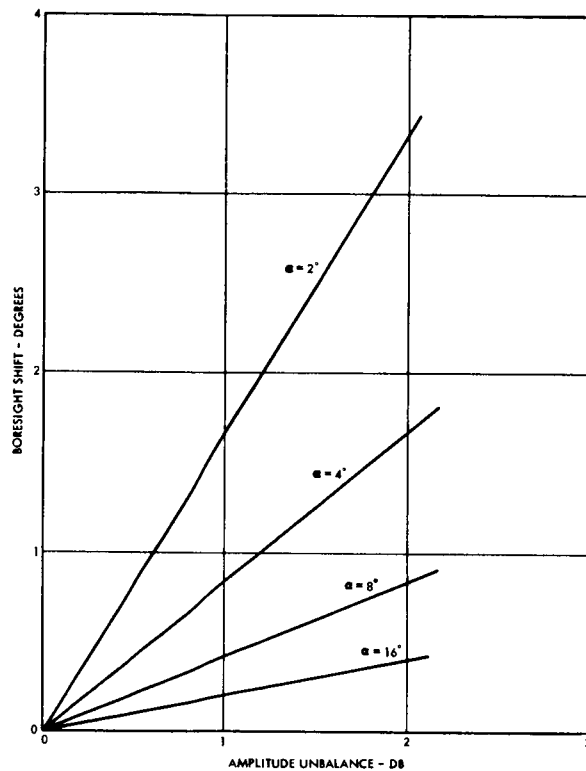
Figure 5. Boresight Shift vs Unbalance
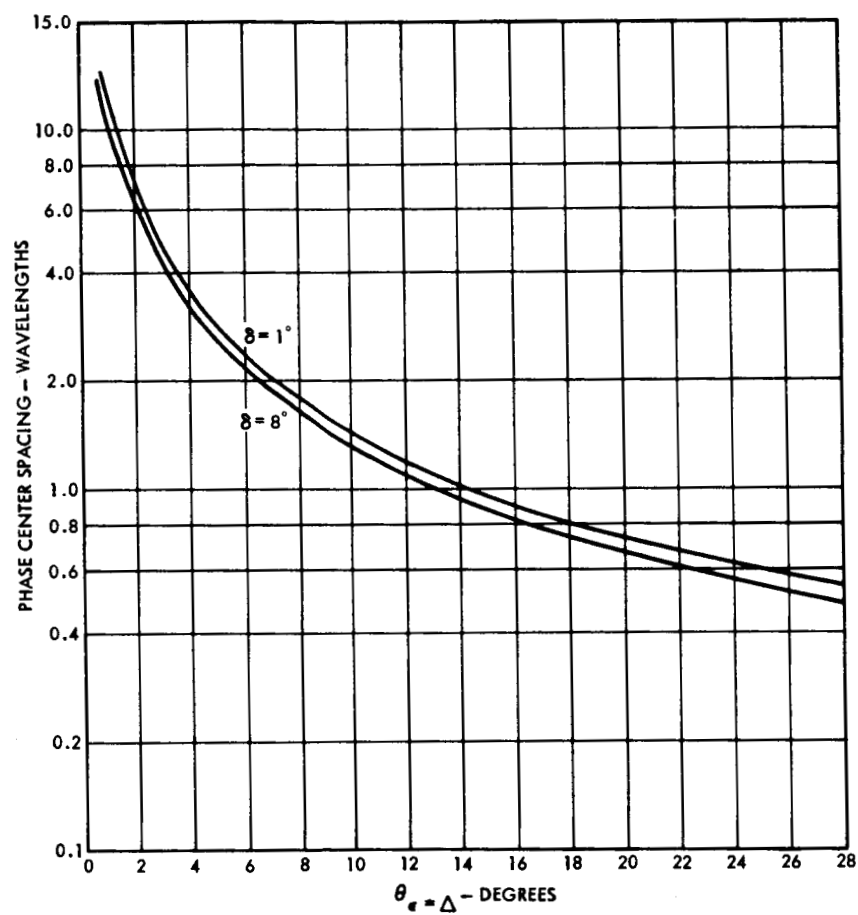for Amplitude Comparison System

Figure 6.   Center Spacing vs Steering Angle
at $E_{\Sigma} = E_{\Delta}$

the feed are available, it is more accurate to use the appropriate beam deviation factor[4] for the parabola with the phase center offset from the focal point.

---

[4]Lo, Y. T., "On the Beam Deviation Factor of a Parabolic Reflector," Trans. on Antenna and Propagation, Vol. AP-8, No. 3, May 1960.

3. MODULATION ANALYSIS OF THE LEM
RF TRACKING ANTENNA

3.1 DESCRIPTION

An automatic tracking capability has been added to the LEM communication antenna to replace the IR tracker originally planned for pointing the antenna earthward. The system design has been modified for antenna lobe switching and extraction of the AGC voltage from the communication receiver for an error signal. The antenna lobe switching amplitude modulates the received signal which ideally has no effect on the information channel which is phase modulated. This analysis is concerned with the antenna parameters which cause residual phase modulation. First, the operation of the antenna will be described; then a mathematical model will be derived which will serve to calculate the amplitude and phase modulation. The concluding portion of this section is computer solutions of the modulation equation using LEM parameters and several variations to demonstrate the sensitivity of certain parameters.

3.2 ANTENNA OPERATION AND CHARACTERISTICS

The LEM antenna consists of a single parabolic reflector with five separate feeds. A turnstile antenna in front of a ground plane is used to obtain the "sum" signal from the parabola. It is phased for right circular polarization. The phase center of the turnstile and its reflection in the ground plane is on the boresight axis at the surface of the ground plane which coincides with the focus of the parabola. The difference signals are obtained from two pairs of radial slots cut in the ground plane. The phase center of each slot does not coincide with the turnstile phase center so that the antenna does not operate as a pure amplitude monopulse antenna.

The beam of the turnstile is alternately switched off axis in the azimuth plane and the elevation plane by adding the attenuated difference signal in each plane to the turnstile signal in sequence.

This switching action produces amplitude modulation which, after decommutation, generates steering error signals for the azimuth and elevation servos.

The principle behind an automatic tracking antenna is the comparison of the received signal between two antennas in each plane. The comparison may be either amplitude or phase. The LEM antenna is primarily an amplitude comparison device in which the signal from any direction except boresight varies in amplitude, but not in phase, as the lobe is switched. If the phase centers of the two feeds coincided, no phase modulation would be produced. The displacement of the phase centers and phase errors in the microwave network are the main source of residual phase modulation. Figure 7 shows a schematic drawing of the LEM antenna with the parameters dimensioned.

Figure 7. LEM Antenna Parameters
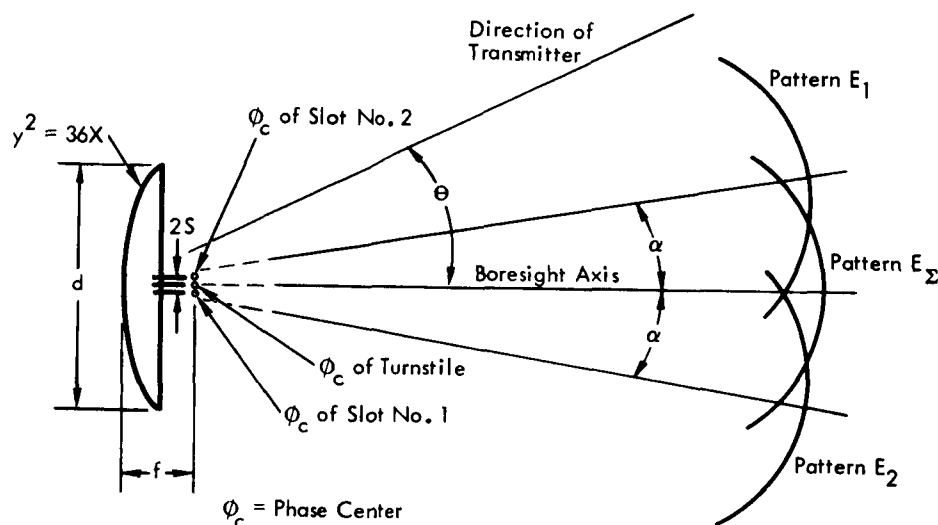
The pattern of the turnstile can be represented closely by the following function

$$E_{\Sigma} = \frac{\sin k\theta}{k\theta}$$

where

E_{Σ} = voltage at terminals of turnstile from excitation in one polarization

k = angular scale factor

θ = steering error angle

The patterns of the two slot radiators are squinted to the right and left and can be represented mathematically by

$$E_1 = \frac{\sin k(\theta - \alpha)}{k(\theta - \alpha)} \, e^{-i\varphi}$$

$$E_2 = \frac{\sin k(\theta + \alpha)}{k(\theta + \alpha)} \, e^{i(\varphi + \delta)}$$

where

α = squint angle

φ = phase error due to phase center displacement "S"

    = $2\pi S/\lambda \sin \theta$

λ = wavelength

δ = phase error in microwave network

The difference signal is obtained by subtracting E_2 from E_1.

$$E_\Delta = E_1 - E_2$$

The shifted lobe is obtained by attenuating E_Δ and adding it to E_Σ.

$$E_s = E_\Sigma + CE_\Delta$$

Addition in this equation produces a radiation lobe shifted to the right, or $+\theta$ while subtraction would shift to the left. For this analysis it will be assumed that the shift is toward $+\theta$.

The attenuation of the difference signal is required to optimize the tradeoff between angular range and error sensitivity. Phase modulation may be found from the difference in the argument of E_s and E_Σ.

$$PM = \text{Arg } E_s - \text{Arg } E_\Sigma$$

$$AM = \frac{|E_s| - |E_\Sigma|}{|E_s| + |E_\Sigma|}$$

The Design Review[5] gives enough data so that the above equations

[5] Design Review No. 1 Report on the LEM S-Band Steerable Antenna Assembly, Volume I, Document R 2950-3891: Dalmo-Victor Company.

may be solved.

From the 3 db beamwidth of the receiving antenna which is 13.7°
(page 2-117)

$$E_\Sigma = \frac{\sin k\theta}{k\theta}$$

$$0.707 = \frac{\sin k\theta \ 3 \ db}{k\theta \ 3 \ db}$$

$$k\theta_{3\ db} = 1.39$$

$$k = \frac{1.39}{13.7° \times 1/2}$$

$$k = 0.203 \text{ for } \theta \text{ in degrees}$$

The squint angle can be found from the drawings 101390 and 101391
which show the feed and parabola dimensions

$$\alpha = 0.8 \tan^{-1} \frac{1.54"}{9"} = 7.75°$$

where

$\quad\quad 0.8 = $ beam deviation factor for parabola with f/d
$$= 9/26 = 0.346[6]$$

$\ 1.54" = $ distance from focus to center of slot

$\ 9.0" = $ focal length of parabola

It can be seen that the point where $E_\Sigma = E_\Delta$ is determined by a zero
of one of the element patterns because the squint angle is greater than
half the beam width. The phase center spacing curve in Section 2 does
not apply and S must be obtained from physical dimensions.

The value for phase center displacement is approximately the
distance from the focus to the center of the slot because as a radiator
moves normally to the axis of a parabola away from the focus, the closer
side of the parabola will induce more current than the opposite side,

---

[6] Lo, Y. T., On the Beam Deviation Factor of a Parabolic Reflector,
Trans. on Antenna and Propagation, Vol. AP-8, No. 3, May 1960, p. 347.

shifting the phase center of the secondary pattern off the axis in the same
direction as the radiator. The value of S will be taken as 1.54 inches
(3.91 cm) and the value of λ is 14.273 centimeters for the receiving
frequency.

The null depth vs phase error curve in Section 2 can be used to
determine δ. The null is 33 db below the peak of E_Σ; therefore, the
phase error is 2-1/2°.

To establish the value of C, two points on the measured antenna
patterns were selected which are equally spaced around the boresight
and the fractional value CE_Δ found which added to E_Σ produces the
correct value of E_s as shown on the measured antenna pattern, pages
2-121. At $\pm 10^\circ$ it was found that 0.44 E_Σ had to be added to and sub-
tracted from E_Σ, to produce E_s. Using the parameters determined
thus far the sum and difference levels can be related to each other by
solving the equations for the sum and difference levels and setting the
absolute value of CE to equal 0.44 E_Σ. From this it was found that C
equals -13 db which is the value given in the Theory of Operation.[7] This
coincidence indicates that the turnstile and slots have the same efficiency.

Solutions of the above equations are very tedious if done manually
for more than a few points. The TRW "on-line" computer[*] was pro-
grammed to solve the equations digitally at 127 points within an
appropriate range of steering error angle.

The final results show AM and PM on an oscilloscope display.
However, the curves of any value in the computation can also be displayed.
By checking the shape of the antenna patterns one can be assured that the
correct constants were used in the original equation. Figure 8 shows a
sample of the sum, attenuated difference, and shifted patterns. These

---

[7] "Theory of Operation of the Microwave Earth Station Tracker for the
LEM S-Band Steerable Antenna," Dalmo Victor Company, R-2950-3774,
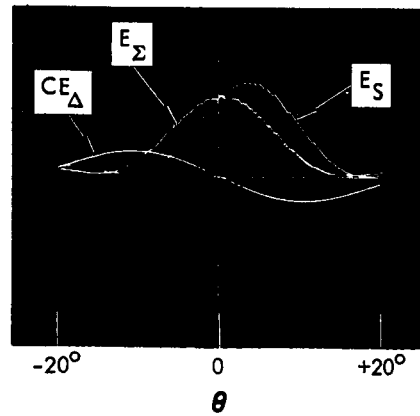9 April 1965.

[*] See Appendix C for brief description.

Figure 8. Computer Antenna Patterns for LEM

curves are in absolute value and do not show phase as in the actual antenna patterns. The roughness is due to computer roundoff of the sin x/x function. It is interesting to note that the peak of the difference curve occurs at 10° for a squint angle of 7.75^o. This coincides with the actual patterns of the antenna mockup.

Figure 9 shows the AM produced by switching from E_Σ to E_s with two values of attenuation for the difference signal. The slope for 13 db is 4 percent per degree. The asymmetry is caused by the non-symmetrical beam switching. Figure 10 shows the phase modulation between E_Σ and E_s at the same two levels of attenuation. The value is under 10 electrical degrees of phase modulation between -10 degrees and +13 degrees bearing error angle. The beam is switched in the positive direction from boresight.

Figures 11 and 12 show AM and PM for variation in the inter-connecting network producing the difference signal. This is the quantity which determines the null depth of the difference signal at boresight.

Figures 13 and 14 show effects of varying the squint angle. This effect would result from varying the spacing between the slots.

Figure 15 shows an expanded scale of PM and AM for the best available parameters for LEM.

3.3 CONCLUSION

The specification calls for less than $\pm 2.50^o$ phase modulation during normal tracking. The quantity of phase modulation goes through zero at boresight with a slope less than 1° PM per degree error angle. Normal tracking is usually less than $\pm 1^o$ error during fluctuation and therefore meets the specification. Acquisition angle of $\pm 15^o$ is doubtful because PM becomes excessive beyond 10° on the negative side and 14° on the other. Phase reversal of the error signal occurs at 12° and 16°.

Increasing the attenuation of the difference signal decreases the PM from 8° to 13° on the negative side of boresight, but has almost no effect on the other side. AM sensitivity decreases as the attenuation increases.

+100%

AM   0

-100%

α = 7.75°
C = 13db and 16db
δ = 0

16db

13db

-20°   0   + 20

θ
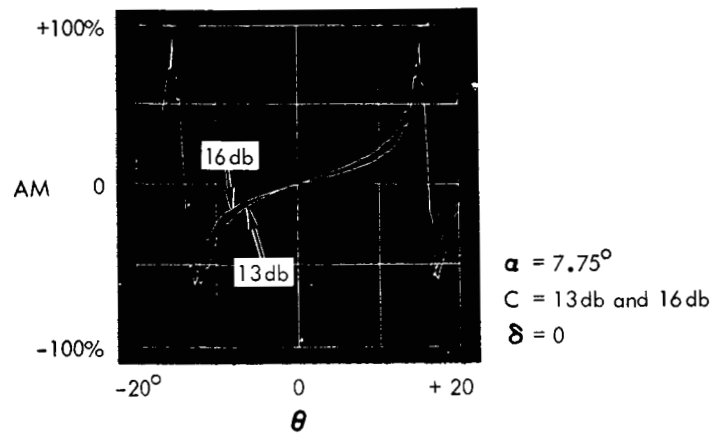
Figure 9. AM with C=13 and 16 db

+200°

PM   0

-200°

α = 7.75°
C = 13db and 16db
δ = 0

16db

13db

-20°   0   +20°

θ
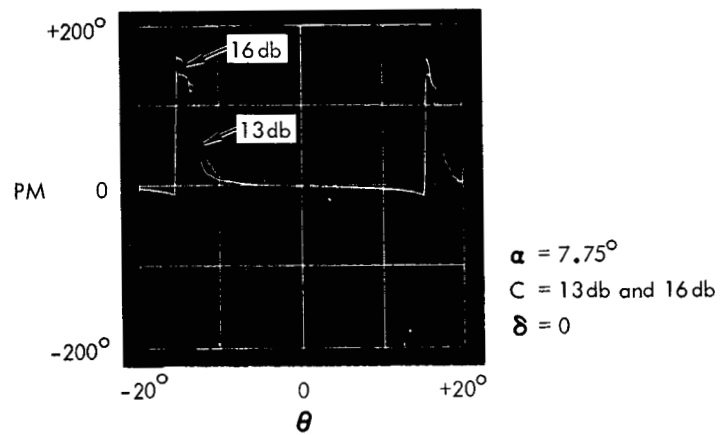
Figure 10. PM with C=13 and 16 db

-20-
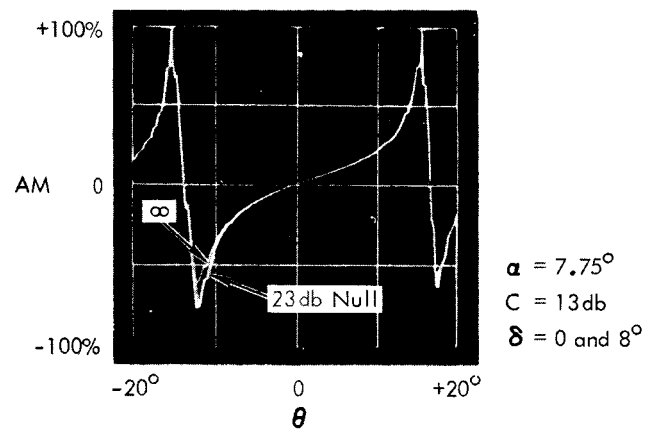
Figure 11. AM with Infinite Null and 27 db Null
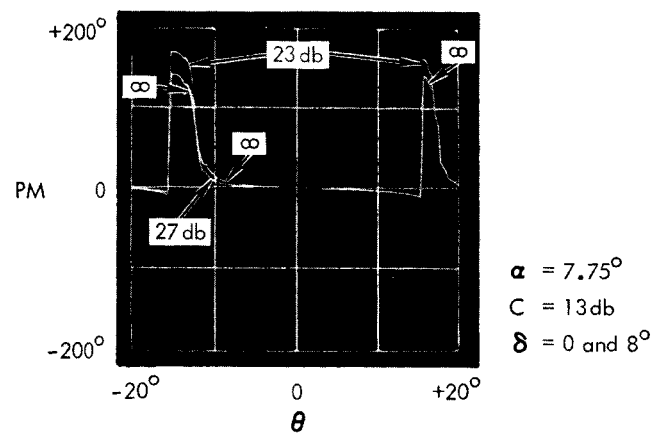
Figure 12. PM with Infinite Null and 27 db Null

-21-
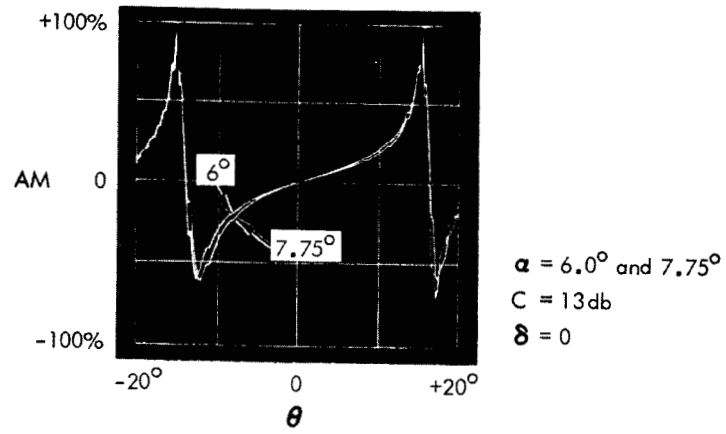
Figure 13. AM for Variation in Squint Angle
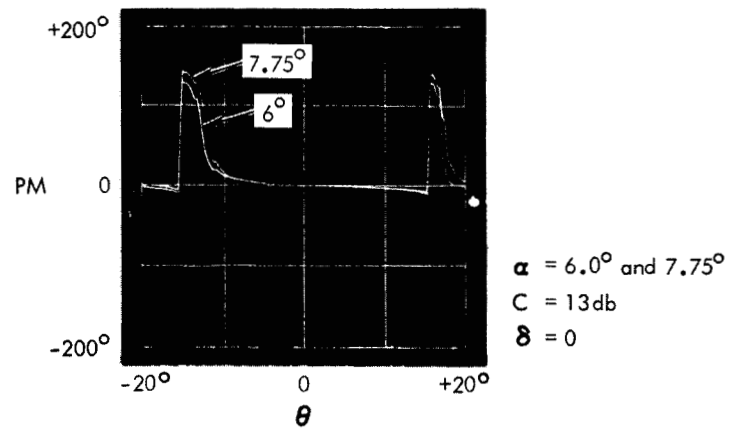
Figure 14. PM for Variation in Squint Angle
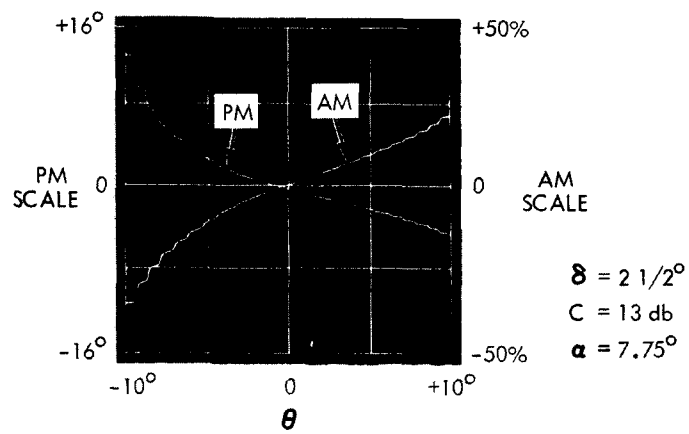
Figure 15. Expanded PM and AM

Improving the null depth has negligible effect on the amount of AM, but increases the PM on the negative side of boresight. A 23 db null depth is equivalent to 8 electrical degrees error in the connecting network. Physically this error represents about 3 mm or 1/8 inch accumulation of errors in the microwave network.

The squint angle was also varied to check its effect on operation. The angle was decreased from 7.75° to 6° and the PM improved slightly at the expense of reduced AM sensitivity.

4. MODULATION ANALYSIS OF THE CSM RF TRACKING ANTENNA

An automatic tracking capability has been added to the CSM communication system by modifying the antenna for lobe switching and extraction of an error signal from the communication receiver AGC circuit. The lobe switching adds amplitude modulation to the received signal which ideally has no effect on the information channel which is phase modulated. This analysis is concerned with the source of residual phase modulation introduced by the lobe switching circuits.

The following paragraphs will explain the operation of the lobe switching antenna system and show how the modulation, both AM and PM, can be related to physical parameters. The concluding portion of this section shows computer solutions using values typical for the wide and narrow beam CSM antenna.

The CSM communication antenna consists of four parabolas with four turnstiles at the center which provide three modes of operation. The four parabolas are used as an array for narrow beamwidth or singly for medium beamwidth. The wide beam mode utilizes the four turnstiles on a ground plane located in the center of the four parabolas.

RF tracking is used only in the narrow and wide modes in which four parabolas or four turnstiles are used to obtain angle sensing information. Both the narrow and wide mode tracking systems operate in a similar way so that one error analysis will serve for both modes of operation.

The four parabolas or turnstiles are connected to a microwave network consisting of four $180°$ hybrids which combine the four input signals to produce a sum signal, an elevation difference, and an azimuth difference signal.

The difference signals are attenuated and added in phase or out of phase with the sum signal so that the main beam is alternately switched up, down, left, and right of the boresight direction. Attenuation is required to optimize the tradeoff between angular range and error sensitivity. For purposes of analysis, it is sufficient to consider the

problem in one plane only. The switching action modulates the amplitude envelope of the received signal which may be recovered by sampling the unfiltered AGC circuit.

The narrow mode antenna is a phase comparison antenna because the individual feeds are 5-1/2 wavelengths apart. With such a large separation, the relative phase of the two antennas changes rapidly with direction while the amplitude difference is about constant. The feed of each dish is tilted slightly to broaden the main beam but the phase center of the feed is at the focus of the parabola. This method of feed causes non-uniform illumination of the parabola which squints the beam slightly and makes the side lobes higher and nonsymmetrical. The predominant effect is the separation of phase centers which makes the system a phase comparison system.

The wide mode antenna requires closer examination of the data to decide whether it is an amplitude or phase comparison antenna. The nonsymmetrical surrounding of each element may lead one to believe the individual beams are squinted. However, the elements are 6.4 centimeters apart which is approximately a half wavelength. The sum and difference patterns shown on page 57 of the Final Report[8] show that the two values are equal at $\pm26°$ off boresight. If the antennas are primarily amplitude comparison, a null at $26°$ in each pattern is required. This seems unlikely unless the two elements were driven with equal amplitude and a phase relationship to produce the null. If the antennas are phase comparison, the vector relationship between the individual voltages at $\theta = 26°$ must be $\pi/4$. When two equal length vectors result from adding and subtracting two equal length vectors, a quadrature relationship is required between each pair of vectors. In our case the antenna voltages are $+45°$ and $-45°$ for this to be true. The phase φ can be shown to be equal to $2\pi S/\lambda \sin \theta$. Solving this for S results in the following

---

[8] "RF Earth Sensor 60-Day Study Final Report for Apollo CSM High Gain Antenna," Dalmo Victor Report R-3028-3953, 14 October 1965.

$$\pi/4 = \frac{2\pi S}{\lambda} \sin \theta$$

$$S = \frac{\lambda}{8 \sin \theta} = \frac{14.273}{8 \sin 26^\circ} = 4.05 \text{ cm}$$

The effective spacing between elements is 2S or 8.1 cm which is 25% higher than the actual value of 6.4 cm. The increased spacing is probably caused by reflections in the shield box around the radiators.

The final clue that indicates the wide mode antenna is a phase comparison system which is indicated by the level of the $E_\Sigma = E_\Delta$ points relative to the $E_{\Sigma \text{ max}}$ point. The average of the right and left points is 3-3/4 db below the peak of the sum pattern. Using the parameters for the wide mode antenna results in the following calculation for the level of the $E_\Sigma = E_\Delta$ point: assuming a pure phase comparison antenna:

$$\frac{E_{\Sigma_{26}}}{E_{\Sigma_0}} = \frac{\dfrac{\sin\left(\dfrac{1.54 \cdot 26}{57.3}\right)}{0.7} \angle 45^\circ + \dfrac{\sin(0.7)}{0.7} \angle -45^\circ}{2 \angle 0}$$

$$= \frac{\sqrt{2}\,(0.9203)}{2} = 0.652$$

$$= -3.72 \text{ db}$$

Assuming that both antennas are phase comparison devices, the same analysis will serve for both. Individual antenna patterns can be closely approximated by the following equations

$$E_1 = \frac{\sin k (\theta - \alpha)}{k (\theta - \alpha)} e^{-i\varphi}$$

$$E_2 = \frac{\sin k (\theta + \alpha)}{k (\theta + \alpha)} e^{i(\varphi + \delta)}$$

where

$\quad$ k = angular scale factor

$\quad$ θ = steering error angle

α = squint angle

φ = phase function = $2\pi S/\lambda \sin \theta$

S = spacing of the phase centers

λ = wavelength

δ = pre-comparator phase error

The microwave network performs an addition and subtraction such that

$$E_\Sigma = E_1 + E_2$$

$$E_\Delta = E_1 - E_2$$

The PIN diode switches and their associated networks perform another addition and subtraction, and

$$E_R = E_\Sigma + iC E_\Delta$$

$$E_L = E_\Sigma - iC E_\Delta$$

where

E_R = beam shifted to the right

E_L = beam shifted to the left

The i term in the above equation is in reality a transmission line 90 electrical degrees long. The C term is an attenuation term required to optimize the tradeoff between angular tracking range and error signal sensitivity.

The values for PM and AM are found from the above equations by performing the following operations

$$PM = \text{Arg } E_R - \text{Arg } E_L$$

This is simply the phase difference between the two vector quantities disregarding their magnitude. Amplitude modulation is found from the absolute magnitudes

$$AM = \frac{|E_R| - |E_L|}{|E_R| + |E_L|}$$

This analysis is essentially the same as the LEM analysis in Section 3 except for the addition of the i term in determining E_R and E_L and in the detail of determining PM and AM. This latter exception comes about because the LEM is a nonsymmetrical system while the CSM is balanced.

Using values obtained from the antenna patterns and text of the Final Report, the following values were determined for each antenna

Quantity	Wide	Narrow
S	4.05 cm	38.5 cm
k	1.54	12.9
C	-4.2 db	-19.1 db

These values and assumed values of α and δ were programmed for the TRW on-line computer[*] to solve for AM and PM over appropriate ranges of θ for each antenna system.

Figures 16 and 17 show PM and AM for the wide mode antenna at various squint angles. For 0° squint no PM is produced until 38° off boresight is reached. At that point, the phase reverses. Changing the squint angle has only a minor effect on error signal sensitivity.

Figures 18 and 19 show PM and AM at two values of the coupling factor C. As the coupling factor is reduced (higher db) the error signal sensitivity is reduced and the PM is lower. Figures 20 and 21 are expansions of the PM and AM around the boresight axis.

Figures 22 and 23 show PM and AM with several values of difference signal null depth. The values of δ selected, 0°, 8°, and 10° correspond to an infinite null, a 27 db null, and a 25 db null. The AM curve shows that this quantity moves the zero error position about 5° off boresight.

Figures 24 and 25 show expansions of the AM and PM near boresight with finite nulls in the difference pattern and a small amount of squint angle.

---

[*]See Appendix C for brief description.
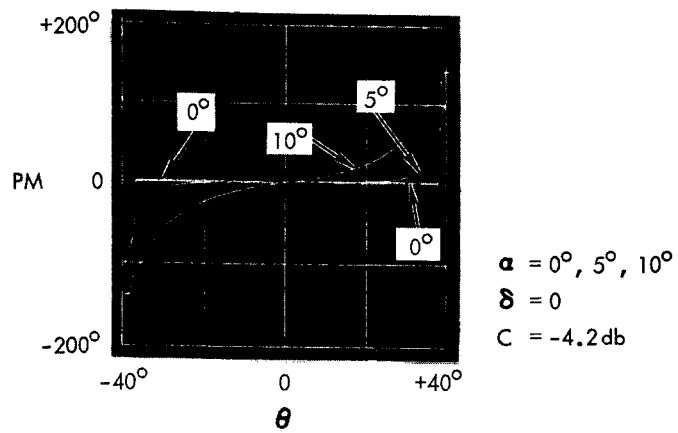
Figure 16. Wide Mode PM with Various Squint Angles

$\alpha = 0°, 5°, 10°$
$\delta = 0$
$C = -4.2$ db
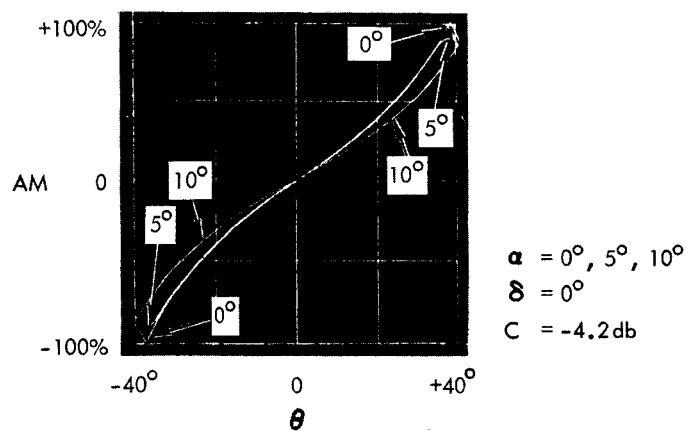
Figure 17. Wide Mode AM with Various Squint Angles

$\alpha = 0°, 5°, 10°$
$\delta = 0°$
$C = -4.2$ db

Figure 18. Wide Mode PM with Various Coupling Factors

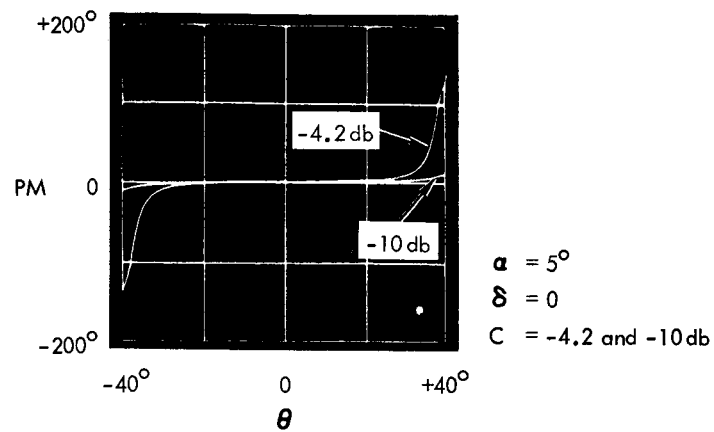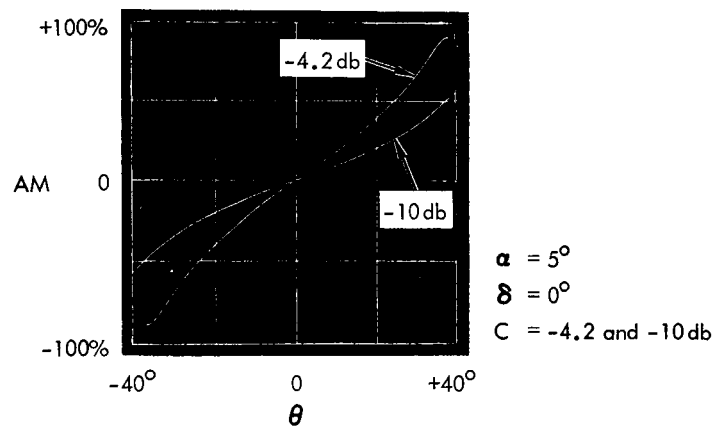Figure 19. Wide Mode AM with Various Coupling Factors

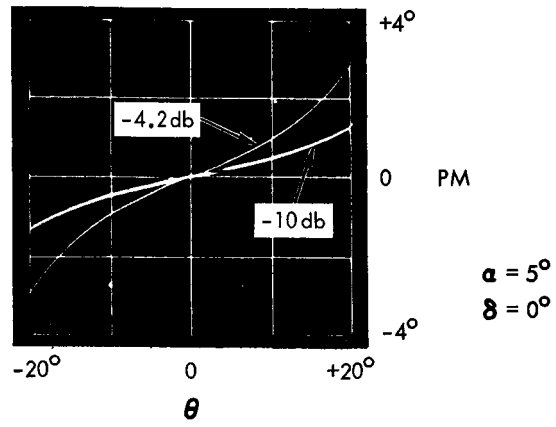Figure 20. Expanded PM
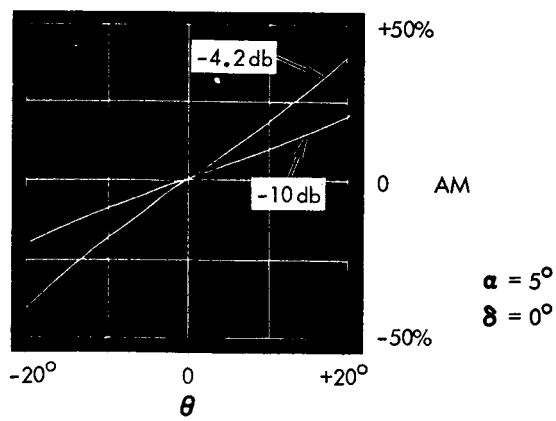
Figure 21. Expanded AM
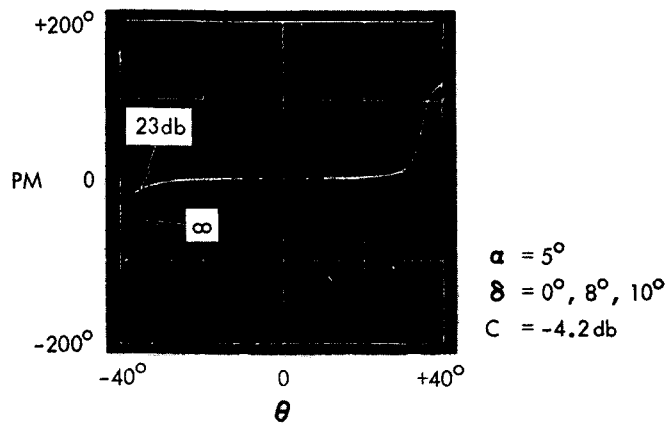
Figure 22. Wide Mode PM with Various Null Depths
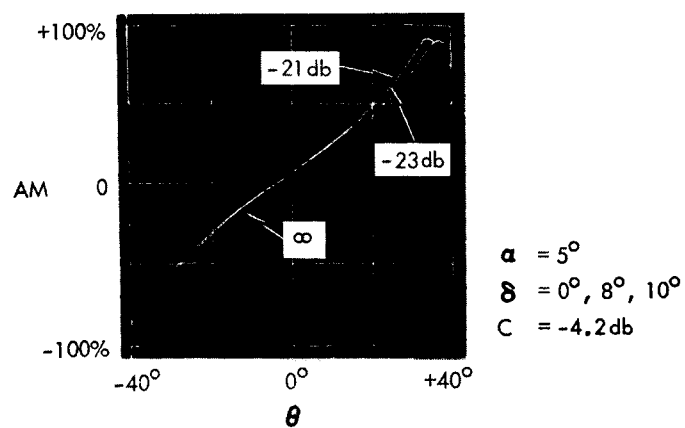
Figure 23. Wide Mode AM with Various Null Depths
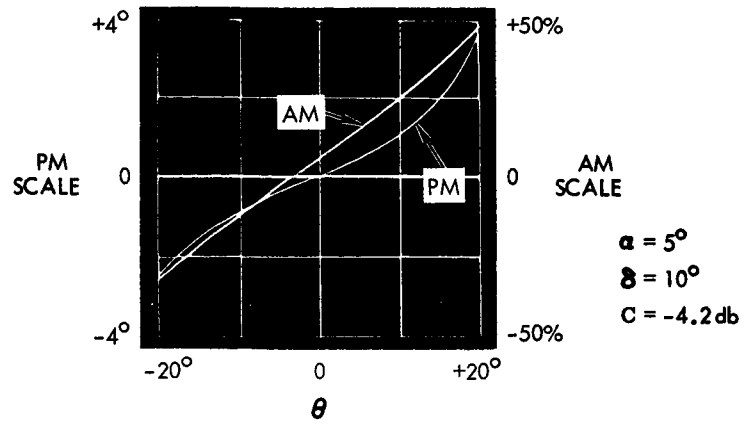
Figure 24.   Wide Mode Expanded Scale for $\alpha = 5^\circ$
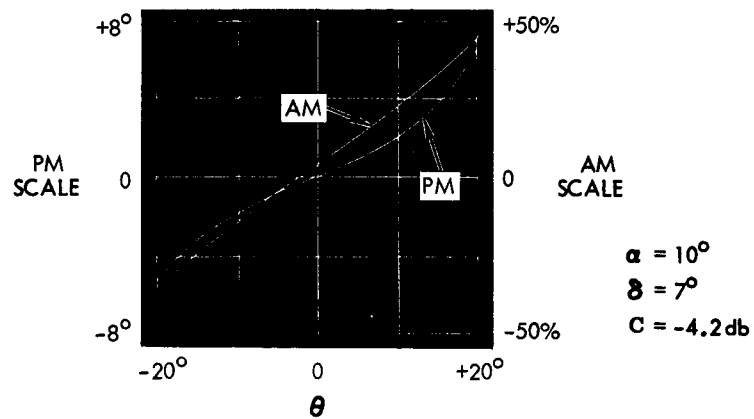
Figure 25.   Wide Mode Expanded Scale for $\alpha = 10^\circ$

The CSM narrow mode results are shown in the final set of figures starting with Figure 26.

Figures 26 and 27 show the AM and PM for various squint angles. It can be seen that the slope of the error signal (AM) near boresight does not change with squint angle. The peak near the extreme of the tracking range, peaks up sharply with 0° squint and is nearly linear at 2° squint. The appearance of the error signal in the Final Report (page 34) suggests that the actual squint angle in the mockup must have been about $1/2^\circ$ because the AM peaks up to about 80 percent while the calculations show 100 percent at 0° squint and 50 percent at 1° squint angle.

It should be noted that the 180° phase reversal occurs only in the region of null overlap between the main beam and the first sidelobe. This region is unstable because the error signal is reversed. Steering angles which are in the side lobe produce correctly phased error signals for tracking in the center of the side lobe.

Figure 28 is an expansion of Figure 27 which shows greater detail of phase modulation near boresight. For $1/2^\circ$ of squint angle, about 5° of PM is generated at 4° off boresight.

Figures 29 and 30 show PM and AM with increased coupling factor and 3 values of squint angle.

The error signal sensitivity is increased but the PM is increased also. The tracking range is decreased from $\pm 4.8^\circ$ to $\pm 4.2^\circ$ for zero squint angle.
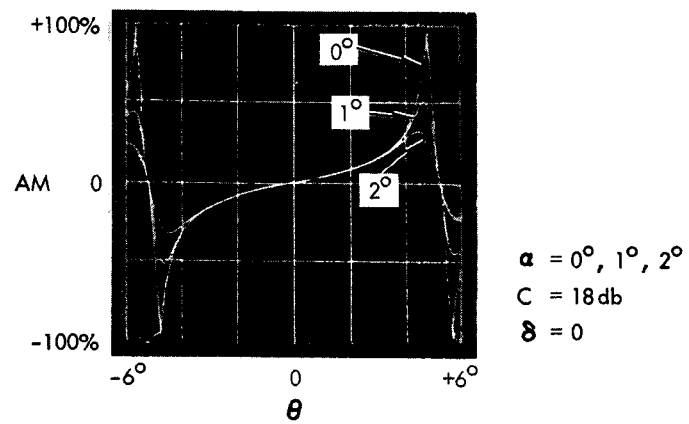
Figure 26. Narrow Mode AM at Several Squint Angles
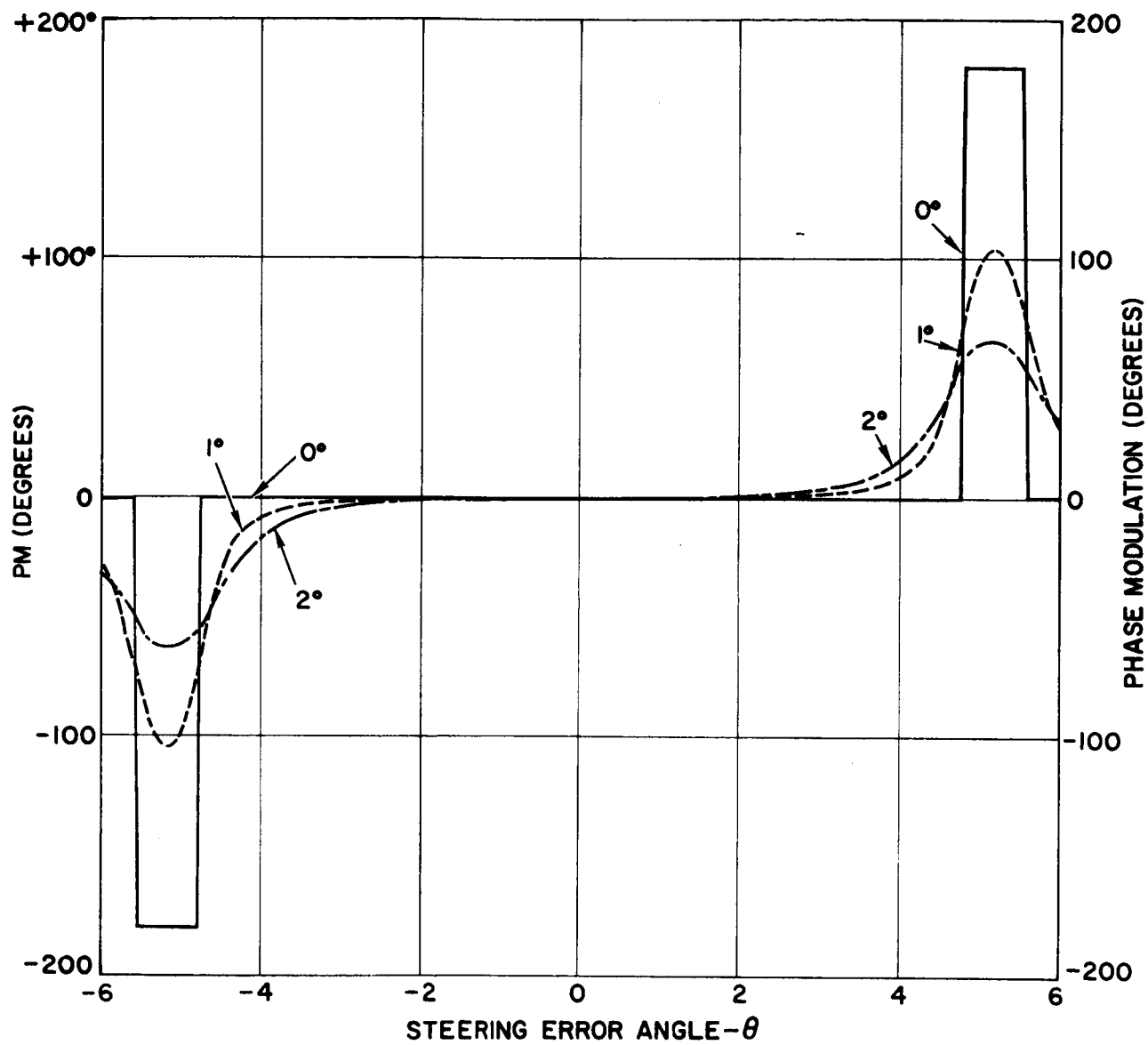
Figure 27. Narrow Mode Phase Modulation
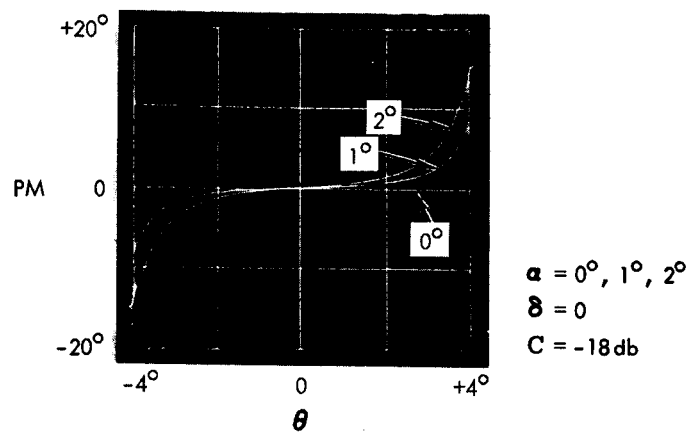
Figure 28. Narrow Mode Expanded PM
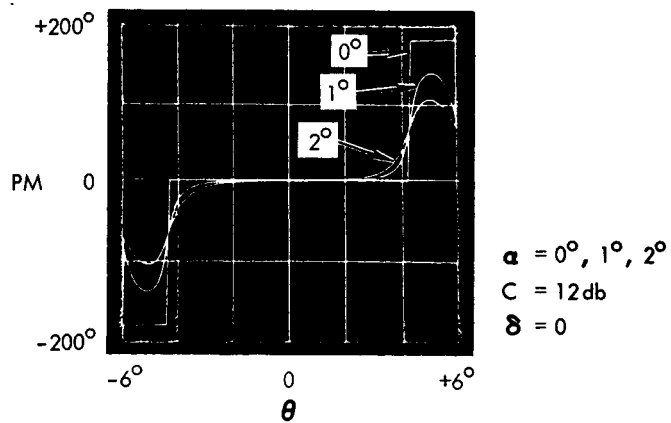
Figure 29. Narrow Mode PM with Increased Coupling Factor
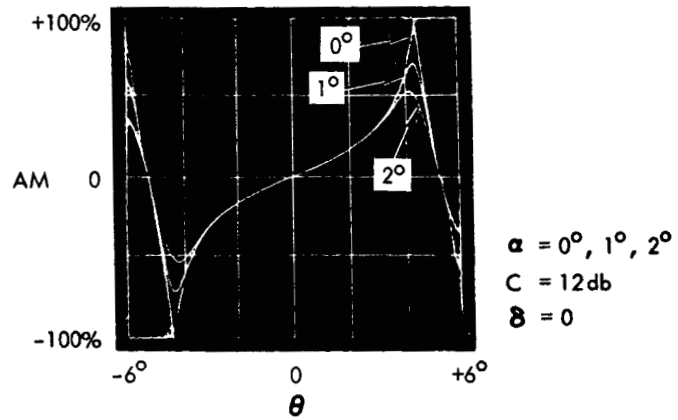
Figure 30. Narrow Mode AM with Increased Coupling Factor

5. THE EFFECTS OF THE RF ANTENNA TRACKING SYSTEM ON COMMUNICATIONS

The effects of the RF antenna tracking system on communications are most readily seen by considering the action of the antenna tracking system. For a two dimensional analysis of the CSM, the antenna array of the antenna tracking system can be represented as shown in Figure 31.
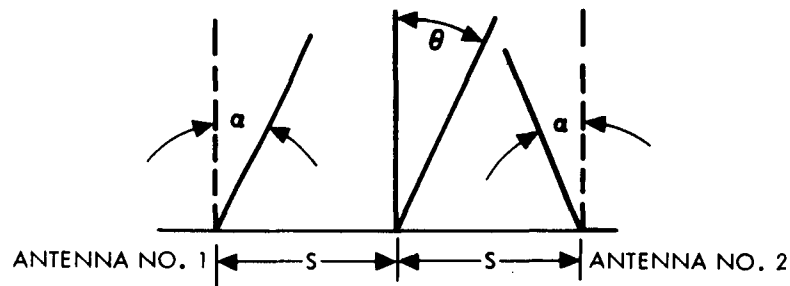
Figure 31. Tracking Antenna Array

Let

$$E_1 = \text{signal from Antenna No. 1}$$

$$E_2 = \text{signal from Antenna No. 2}$$

The magnitudes of the signals can be expressed as

$$\left| E_1 \right| = A (\theta - \alpha)$$

$$\left| E_2 \right| = K A (\theta + \alpha)$$

where α = the amount of squint of the antennas toward boresight. This value may differ from the actual squint angles since the actual arrays are four element arrays, each element of which may not be squinted in the planes of the control axes. The squint angle may also appear as a result of mutual impedance between the antennas.

Because of the physical spacing of the antennas, the signals become

$$E_1 = A(\theta - \alpha)e^{-i\varphi} \tag{1}$$

$$E_2 = KA(\theta + \alpha)e^{i(\varphi + \delta)} \tag{2}$$

where

$$\varphi = 2\pi \frac{S}{\lambda} \sin \theta \tag{3}$$

= phase relative to the center
of the array

δ = phasing error

The sum signal is

$$E_\Sigma = E_1 + E_2$$

$$= A(\theta - \alpha)e^{-i\varphi} + KA(\theta + \alpha)e^{i(\varphi + \delta)} \tag{4}$$

The difference signal is

$$E_\Delta = iC(E_1 - E_2)$$

$$= iC\left((A(\theta - \alpha)e^{-i\varphi} - KA(\theta + \alpha)e^{i(\varphi + \delta)}\right) \tag{5}$$

C is the attenuation coefficient $(0 < C \leqq 1)$.

Defining the null depth as

$$\text{Null depth (db)} = D = 10 \log \frac{|E_\Sigma|^2}{|E_\Delta|^2} \quad \text{on boresight} \tag{6}$$

for $|\delta| << $ radian

$$\frac{|E_\Sigma|^2}{|E_\Delta|^2} = 10^{\frac{D}{10}} \cong \frac{(K+1)^2}{C^2(K-1)^2}$$

and K can be related to null depth and difference signal attenuation by

$$K = \frac{10^{\frac{D}{20}} C \pm 1}{10^{\frac{D}{20}} C \mp 1} \tag{7}$$

The $\pm$ signs are used because a null depth measurement alone will not indicate whether $|E_2|$ is larger or smaller than $|E_1|$ on boresight.

The signal resulting from shifting the beam to the right is

$$E_R = E_\Sigma + E_\Delta$$

$$= \sqrt{1 + C^2} \left[E_1 e^{i \tan^{-1} C} + E_2 e^{-i \tan^{-1} C} \right] \tag{8}$$

and the left-shifted signal is

$$E_L = E_\Sigma - E_\Delta$$

$$= \sqrt{1 + C^2} \left[E_1 e^{-i \tan^{-1} C} + E_2 e^{i \tan^{-1} C} \right] \tag{9}$$

The antenna tracking system is a phase monopulse-type system using one channel in time division multiplex, hence the input to the transponder receiver can be represented as

$$v(t) = \begin{cases} \text{Re} \left[E_R e^{i(\omega_c t + \theta_c)} \right] & 0 \le t < T \quad \text{mod } 2T \\ \text{Re} \left[E_L e^{i(\omega_c t + \theta_c)} \right] & T \le t < 2T \quad \text{mod } 2T \end{cases}$$

which is, in general, both amplitude and phase modulated. Using the expressions above for E_1, E_2, E_R, and E_L, the following expressions for AM and PM near boresight are easily derived (Appendix A).

-42-

$$\text{AM (percent)} = \frac{|E_R| - |E_L|}{|E_R| + |E_L|} \, (100)$$

$$= 2\pi \frac{S}{\lambda} \, C(\theta + \theta_S) \, (100)$$

(10)

$$\theta_S = \text{boresight shift}$$

$$= \frac{\delta}{4\pi \frac{S}{\lambda}}$$

$$\text{PM (peak-to-peak)} = \text{Arg } E_R - \text{Arg } E_L$$

(11)

$$= \mp \, 2\left(10^{-\frac{D}{20}}\right) + \left[1 + \frac{10^{-\frac{D}{10}}}{C^2}\right]\left[-2\,\frac{A'(\alpha)}{A(\alpha)}\right] C\theta$$

where α and θ are both in radians. The term $A'(\alpha)/A(\alpha)$ is readily related to the slope of the antenna power pattern of the individual antennas within the array.

$$\frac{A'(\alpha)}{A(\alpha)} = \frac{d}{d\theta}\left[\ln A(\theta)\right]\Big|_{\theta = \alpha}$$

$$= \left(\frac{\ln 10}{20}\right) \frac{dG(\theta)}{d\theta}\Big|_{\theta = \alpha}$$

where

$$G(\theta) = \text{antenna power pattern (in db)}$$

$$= 20 \log A(\theta), \; \theta \text{ and } \alpha \text{ in radians}$$

After acquisition, the transponder carrier tracking loop is required to track the uplink carrier and provide a reference for the wideband demodulator. The phase error transfer function of a high gain loop is

$$\frac{\theta_e(S)}{\theta_i(S)} = \frac{S^2}{S^2 + 2\zeta\omega_n S + \omega_n^2}$$

Since the bulk of the spectrum of the incidental PM will be within the loop bandwidth, the loop will track the incidental PM, but the error in tracking the PM, $\theta_e(t)$, will accompany the demodulated PRN code. A good estimate of the phase transients that will accompany the PRN code can be obtained by considering the following expression for $\theta_i(t)$

$$\theta_i(t) = \frac{\Phi}{2} f(t)$$

where

Φ = peak-to-peak incidental phase modulation

$$= \mp 2 \left(10^{-\frac{D}{20}} \right) + \left[1 + \frac{10^{-\frac{D}{10}}}{C^2} \right] \left[-2 \frac{A'(\alpha)}{A(\alpha)} \right] C \theta$$

$f(t)$ = symmetrical unit square wave of period 2T, T = 5 ms

Then

$$\theta_i(S) = \left(\frac{1}{S} - \frac{e^{-ST}}{S} \right) \frac{1}{1 + e^{-ST}}$$

and the phase error is

$$\theta_e(t) = \sum_{n=0}^{\infty} (-1)^n g(t - nT) \tag{12}$$

$$g(t) = \begin{cases} \dfrac{\Phi}{2} \dfrac{1}{a-b} \left[a e^{-at} - b e^{-bt} \right] & 0 \leqq t < T \\[3em] \dfrac{\Phi}{2} \dfrac{1}{a-b} \left[(a e^{-at} - b e^{-bt}) - (a e^{-a(t-T)} - b e^{-b(t-T)}) \right] & t \geqq T \end{cases}$$

For Apollo, the particular values of a and b are

$$a = \zeta \omega_n \left[1 + \sqrt{1 - \frac{1}{\zeta^2}} \right] \cong 4750$$

$$b = \zeta \omega_n \left[1 - \sqrt{1 - \frac{1}{\zeta^2}} \right] \cong 520$$

-44-

$\theta_e(t)$ rapidly approaches the steady state which has peak values of $\pm \Phi$, or peak-to-peak values which are twice the input peak-to-peak values. The loop is heavily overdamped and $\theta_e(t)$ is reduced to about 10 percent of its peak value in about 0.5 ms. As long as Φ is small compared to the PRN modulation index, the effect of the transient-type noise produced by the antenna tracking system will be negligible.

Equation (11) points out the parameters of importance in assuring that the noise produced by the antenna tracking system will be negligible; the product $[-2 A'(\alpha)/A(\alpha)] C$ and the null depth term must be sufficiently small that random excursions from boresight will not disrupt ranging. From the communications standpoint it would be highly desirable to have no incidental PM at all, a condition which can theoretically be achieved by infinite null depths and by reducing the squint angle α to zero since $A'(0) = 0$. Unfortunately, setting the squint to zero introduces another potential hazard. For $\alpha = 0$, the expressions for the right and left shifted signals can be written as

$$E_R = (K+1) A(\theta) e^{i\frac{\delta}{2}} [\cos(\varphi + \frac{\delta}{2}) + C \sin(\varphi + \frac{\delta}{2})][1 + i \frac{K-1}{K+1} \tan(\varphi +$$

$$+ \frac{\delta}{2} - \tan^{-1} C)]$$

$$E_L = (K+1) A(\theta) e^{i\frac{\delta}{2}} [\cos(\varphi + \frac{\delta}{2}) - C \sin(\varphi + \frac{\delta}{2})][1 + i \frac{K-1}{K+1} \tan(\varphi +$$

$$+ \frac{\delta}{2} + \tan^{-1} C)]$$

Although a finite null depth obviates the possibility of exactly bi-phase modulating the uplink signal, for good null depths the PM index can approach $\pi/2$ when the condition $\cos(\varphi + \delta/2) < C \sin(\varphi + \delta/2)$ occurs.

Obviously, the condition which must be met if zero squint is used and high PM indices are to be avoided is

$$C \leq \frac{1}{\tan(\varphi_A + \frac{\delta}{2})}$$

-45-

where

$$\varphi_A = 2\pi \frac{S}{\lambda} \sin \theta_A$$

which, unfortunately, indicates that there is no optimum tradeoff between acquisition range and error sensitivity for zero squint. For nonzero values of α, estimates of $A'(\alpha)/A(\alpha)$ can be obtained from the Dalmo-Victor medium mode antenna patterns: for $0 \leq \alpha \leq 6°$, -1 db/degree is the greatest value of $A'(\alpha)/A(\alpha)$ encountered and taking $C = 0.126$ (18 db attenuation), $D = 33$ db, $\Phi < \pm 0.045 + 1.66\theta$ from Equation (11) in the narrow beam mode. Dalmo-Victor states that the maximum dynamic tracking error will not exceed $0.7°$ (1.22×10^{-2} radians), hence $\Phi < 6.5 \times 10^{-2}$ radians which compares favorably with the smallest uplink PRN index of 0.5. With respect to the PRN case, the ground receiver is basically a correlation device or matched filter in which the local PRN code is multiplied with the received code. Narrowband interference is thereby spread throughout the 2 mc code bandwidth. Subsequent integration or narrowband filters remove most of the interference. With the processing gain thus derived, the PRN code operates successfully against the interference presented to it by the downlink voice and telemetry subcarrier, both of which fall within the PRN spectrum and have power levels which exceed that of the code. Considering the fact that the power level of the phase noise produced by the antenna tracking system is considerably below that of the voice and telemetry subcarriers (the voice and telemetry modulation indices lie between 0.76 and 1.85 while it was pointed out above that the peak phase error does not exceed 0.065 radian), the phase noise will not provide any serious interference with the PRN code.

Range rate is determined by measuring the length of time it takes the biased doppler signal to go through a given number of cycles. The doppler counter is designed for a ± 180 kc doppler (a range rate interval of $\pm 42,100$ ft/sec) biased about a 1 mc standard frequency. Provision is made for readout at nominal intervals of 0.1 second and 1.0 second and for continuous, nondestructive accumulation of range rate data. The following expression for the indicated range rate is derived in Appendix B.

$$\dot{r}_i = \text{indicated range-rate}$$

$$= \frac{2\pi C}{2\omega_c T_c} (N - f_B T_c)$$

$$= \underbrace{\frac{r(t) - r(t - T_c)}{T_c}}_{\text{true range-rate}} - \underbrace{\frac{c\rho}{2\omega_c T_c} [\theta_e(t - \lambda) - \theta_e(t - T_c - \lambda)]}_{\text{range rate-error}}$$

Here, C = velocity of light, $\omega_c/2\pi$ = uplink carrier frequency, N = number of biased doppler cycles counted, f_B = 1 mc bias, T_c = time required to accrue N counts, $\rho = 240/221$, $\theta_e(t)$ = transponder carrier tracking error produced by the antenna system. Using the peak value of $\theta_e(t)$ near boresight derived above, upper bounds on the magnitude of the range-rate error become (Appendix B)

$$|\dot{r}_e| < \begin{cases} 6.2 \times 10^{-2} \text{ ft/sec} & \text{for } 0.1 \text{ second readout interval} \\ \\ 6.2 \times 10^{-3} \text{ ft/sec} & \text{for } 1.0 \text{ second readout interval} \end{cases}$$

In the nondestructive mode, the range-rate error is negligible, since T_c becomes very large and the variation of $\theta_e(t)$ is bounded. The bounds given here are the result of a worst case analysis in that it was assumed that the ground receiver tracks $\theta_e(t)$ and the peak values of $\theta_e(t)$ were used in calculating the bounds. Hence, it is concluded that the antenna tracking system will have a negligible effect on the determination of range-rate.

Since the wide beam null depths indicated in the Dalmo-Victor reports are greater than those for the narrow beam, it is concluded that the antenna tracking system will have negligible effects on the PRN code and range-rate determination after acquisition in both the wide and narrow beam modes. The other communications services are on subcarriers which are sufficiently far removed in the spectrum to be unaffected by the antenna tracking system. It should be pointed out that these conclusions are based upon parametric information obtained from the published

Dalmo-Victor reports and a large variation from the values of the various parameters used here may necessitate a re-evaluation of these conclusions. Specifically, a null depth of 20 db rather than the 33 db used here can increase the peak-to-peak incidental phase modulation near boresight by a factor of 4 or 5. Such an increase would require a more detailed analysis than has been performed here to evaluate the deleterious effects of the antenna tracking system on communications after antenna boresight acquisition.

Figure 32. Simplified Block Diagram

Referring to Figure 32, the output of the transponder IF at the initiation of acquisition can be expressed as

$$v_i(t) = G_{IF} [1 + a f(t)] \sin \{\omega_c t + b f(t) + \theta\}$$

where a and b are the AM and PM modulation indices, respectively, and f(t) is a symmetrical unit square wave of period 2T, T = 5 ms. This signal arises due to the fact that at the initiation of acquisition the ground station will be transmitting an unmodulated carrier (swept in frequency) and the transponder carrier tracking loop will probably not be in lock; hence, there will be no coherent AGC and no control signal for the antenna tracking system.

-48-

The input to the carrier tracking loop is taken to be

$$v_L(t) = \sin\{\omega_c t + bf(t) + \theta\}$$

This expression assumes that limiting reduces the sidebands produced by the residual AM to negligible levels compared to the PM produced sidebands. If there were no PM, it would be necessary to consider the AM sidebands in $v_L(t)$.

The coherent AGC signal before filtering is

$$v_A(t) = 2v_i(t)\sin\psi_{vco}(t)$$

and the control signal before filtering is

$$v_D(t) = f(t)\,v_A(t)$$

Expanding $v_A(t)$ and $v_D(t)$ yields

$$v_A(t) = G_{IF}\,[1 + a\,f(t)]\cos\{\omega_c t + bf(t) + \theta - \psi_{vco}\}$$

$$v_D(t) = G_{IF}\,[a + f(t)]\cos\{\omega_c t + bf(t) + \theta - \psi_{vco}\}$$

The quantity of considerable interest here is ψ_{vco}. It was shown above that after acquisition, $\omega_c t + bf(t) + \theta - \psi_{vco} = \theta_e(t)$, where $\theta_e(t)$ is given by Equation (12). During acquisition, there is some question regarding whether or not the carrier tracking loop will lock on a sideband of the uplink signal. Expanding the input to the loop, we have

$$v_L(t) = \cos b\,\sin(\omega_c t + \theta) +$$

$$+ \sin b \sum_{n=0}^{\infty} \frac{2}{(2n+1)\pi}\,[\sin\{\omega_c t + (2n+1)\,\omega_m t + \theta\} -$$

$$- \sin\{\omega_c t - (2n+1)\,\omega_m t + \theta\}\,]$$

where $\omega_m = 2\pi/2T$. For $T = 5$ ms, the sidebands are 100 cps apart. The expression for the 3 db bandwidth of the loop is

$$f_{3\,db} = \frac{\omega_n}{2\pi} \sqrt{2\zeta^2 + 1 + \sqrt{(2\zeta^2 + 1)^2 + 1}}$$

where

$$\omega_n = \omega_{no} \sqrt{\frac{\alpha}{\alpha_o}}$$

$$\zeta = \zeta_o \sqrt{\frac{\alpha}{\alpha_o}}$$

The loop bandwidth is specified to be 700 cps and the damping to be 0.707 at a loop SNR of 0 db. Hence

$$\omega_n = \frac{700}{1.06} \sqrt{\frac{\alpha}{\alpha_o}}$$

$$\zeta = \frac{1}{\sqrt{2}} \sqrt{\frac{\alpha}{\alpha_o}}$$

and at lunar distance

$$\frac{\alpha}{\alpha_o} = \frac{0.96}{0.17}$$

Substitution of these quantities yields

$$f_{3\,db} \cong 910 \text{ cps}$$

$f_{3\,db}$ increases only slightly at sublunar distances. With a bandwidth as wide as that indicated, it is most probable that the carrier tracking loop will not lock on a sideband during acquisition.

Although the exact action of the carrier tracking loop cannot be predicted accurately, it is possible to consider an extreme case and examine the results. Suppose, for example, the loop locks on a sideband above the carrier and we take

-50-

$$\psi_{vco} = \omega_c t + (m+1)\omega_m t + \theta$$

which would result in large phase errors accompanying the PRN code. The coherent AGC signal before filtering becomes

$$v_A(t) = G_{IF}\{\cos b \cos(m+1)\omega_m t + a \sin b \sin(m+1)\omega_m t\} +$$

$$+ G_{IF} f(t)\{\sin b \sin(2n+1)\omega_m t + a \cos b \cos(m+1)\omega_m t\}$$

$$= G_{IF}\{\sin b \frac{2}{(m+1)\pi} + a.c. \text{ terms}\}$$

Assuming ideal AGC action, we have

$$G_{IF} = \frac{1}{\sin b \frac{2}{(m+1)\pi}}$$

and $v_A(t)$ becomes

$$v_A(t) = \begin{cases} \frac{(2n+1)\pi}{2\sin b}(1+a)\cos\{(n+1)\omega_m t - b\} & 0 \le t < T, \text{ mod } 2T \\ \\ \frac{(2n+1)\pi}{2\sin b}(1-a)\cos\{(n+1)\omega_m t + b\} & T \le t < 2T, \text{ mod } 2T \end{cases}$$

The control signal before filtering is now

$$v_o(t) = \begin{cases} \frac{(2n+1)\pi}{2\sin b}(1+a)\cos\{(n+1)\omega_m t - b\} & 0 \le t < T, \text{ mod } 2T \\ \\ -\frac{(m+1)\pi}{2\sin b}(1-a)\cos\{(n+1)\omega_m t + b\} & T \le t < 2T, \text{ mod } 2T \end{cases}$$

$$= a + a.c. \text{ terms}$$

The significant result of this special case is that the proper antenna tracking control system signal is obtained. (The same result is obtained if lock, on a sideband below the carrier, is considered.)

The danger is that with control signals of the proper sign, the antenna system would slew to the earth station, the sideband to which the carrier tracking loop is locked would disappear (since AM and PM disappear on boresight), the carrier tracking loop would lose lock, and in all likelihood acquisition would have to be re-initiated. However, it should be hastily pointed out that with respect to the incidental PM produced by the antenna tracking system, the carrier tracking loop acts as a modulation tracking loop rather than a modulation restrictive loop, hence the likelihood of locking on a sideband is remote. If there is serious doubt about the carrier tracking loop successfully locking to the carrier during acquisition, the possibility of locking to a sideband can be completely eliminated simply by temporarily suspending lobing during acquisition until the carrier loop has locked to the uplink carrier. In the wide beam mode, there is sufficient margin to achieve carrier lock off boresight for ranges greater than 2000 nautical miles; this must be true or the antenna tracking system will not work. Since there is no error signal (other than noise) provided for the antenna tracking system until the carrier loop has locked, there seems to be little reason for lobing until the carrier loop is in lock. It should be possible to implement the termination of lobing during carrier acquisition automatically by a system which monitors the AGC bus voltage.

The overall effect of the antenna tracking system on acquisition appears to be that of adding the spacecraft antenna slewing time to previous estimates of acquisition. Newman[9] estimates that 8.0 seconds after spacecraft illumination two-way RF lock will have been achieved and 9.0 seconds after S/C illumination all demodulators will be locked. However, in arriving at his acquisition time estimates, Newman assumes that the spacecraft antenna is properly oriented, which will not, in general, be true with utilization of the RF antenna tracking system. Two-way RF lock is achieved in two steps: first, the spacecraft transponder is locked, then the ground receiver is locked. The spacecraft antenna does

---

[9] Newman, R. H., "Typical Acquisition Procedure," Proceedings of the Apollo Unified S-Band Technical Conference, 14-15 July 1965, NASA SP-87, pp. 261-268.

not start its motion toward the line of sight to the earth station until the spacecraft transponder is locked. If the spacecraft antenna has completed its slewing operation by the time the ground receiver is locked, there will be no increase in acquisition time. If the S/C antenna has not settled by the time the ground receiver is locked, there may be an increase in the amount of time for all demodulators to lock due to a temporary S/C antenna pointing loss. Hence, the worst case increase in acquisition time (in keeping with Newman's worst case estimate) is equal to the spacecraft antenna slewing time.

6. LOSSES AND MULTIPATH

The origin of losses which limit the gain of the receiving antenna on the spacecraft due to the addition of RF tracking is associated with the sum and difference network, the frequency sensitive power divider, and the PIN switching network. The sum and difference network causes very low loss, not over 0.1 db. The loss occurs in the conductor and dielectric material which forms the strip line network. The frequency sensitive power divider for the CSM fine mode has a loss of 0.4 db at the receiving frequency while the coarse mode unit losses are approximately 2.0 db. The losses occur in the strip line materials in the unit. The lobing switch with the PIN diodes accounts for another 1.0 db loss. The total losses for the CSM narrow mode antenna are 1.5 db and the wide mode antenna total loss is 3.1 db.

The LEM losses are not given for the sum and difference network, but they can be assumed to be the same as the CSM, 0.1 db. The FSPD is approximately 0.5 db and the lobing switch accounts for another 0.5 db. The total loss due to RF tracking in the LEM therefore is about 1.0 db.

The losses of 1.0 to 1.5 db with the RF tracker are compensated by more accurate antenna pointing when compared to the IR tracker design. The loss of less than 3.0 db would be offset by improved pointing and therefore produces more signal than the IR tracker system.

The effects resulting from the difference in multipath characteristics between the uplink and downlink are caused by elliptical polarization. The analysis made on the CSM and LEM antennas does not account for differences of this sort because it assumes pure linear polarization which is aligned with the elements of the antenna. The analysis also applies to pure circular polarization, in which case the requirement for alignment is eliminated. Elliptical polarization introduces another parameter of orientation. The orientation of the receiving antenna relative to the uplink wave is independent of the orientation of the transmitted wave for the downlink.

Multipath can be analyzed as a second source of signal whose phase and amplitude are different from the direct wave. The amplitude of the signal reflected from any surface is a function of the angle of polarization

relative to the surface. Therefore, the vehicle may be oriented for minimum multipath interference of the uplink while the downlink may have maximum interference.

The effect of the multipath can be catastrophic, i.e., complete cancellation of the wave at the antenna. This case is unlikely with circular or elliptical polarization because both components must cancel simultaneously. However, one or the other may cancel, which would result in a lower signal level.

No data is available to perform a specific analysis in this area. The axial ratio marks on some of the antenna patterns do not indicate the orientation of the wave for maximum and minimum signal level.

7. CONCLUSIONS AND RECOMMENDATIONS

7.1 LEM

The LEM tracking system produces a good AM signal off boresight with low PM. The acquisition region is non-symetrical because of the unbalanced lobe switching. The acquisition region can be increased slightly by reducing the coupling between the difference and the sum signal. Wider acquisition is obtainable with a tradeoff of reduced error sensitivity.

7.2 CSM

The high side lobe level on the narrow mode tracker could cause trouble. A stable null is produced but the signal level is 9 db below the main signal. By squaring up the feeds the main beam can be increased and the side lobes reduced. This reduces the possibility of locking on a side lobe.

7.3 RESULTS AND CONCLUSIONS

1) $\quad$ AM (percent) $= 2\pi \frac{S}{\lambda} (\theta + \theta_s)(100)$, $\theta \ll 1$ radian $\qquad$ (10)

$$\theta_s = \text{boresight shift} = \frac{\delta}{4\pi \frac{s}{\lambda}}$$

2) $\quad$ PM(peak-to-peak) $= \mp 2(10^{-\frac{D}{20}}) + \left[1 + \frac{10^{-\frac{D}{10}}}{c^2} \right]$

$$\left[-2 \frac{A'(\alpha)}{A(\alpha)} \right] c\theta , \quad \theta \ll 1 \text{ radian} \qquad (11)$$

D = null depth (db)

C = difference signal coupling factor

$\dfrac{A'(\alpha)}{A(\alpha)}$ = related to slope of individual antenna patterns

3) Expression for transponder carrier tracking loop error is given by Equation (12) for square wave incidental PM.

4) Transponder carrier tracking loop is heavily overdamped. Carrier tracking error $\theta_e(t)$ is reduced to about 10% of its peak value in about 0.5 ms.

5) The parameters of importance in keeping IPM small are the null depth D and the product

$$-2 \left[\frac{A'(\alpha)}{A(\alpha)} \right] C \quad \text{(see Equation (11))}$$

6) For zero squint ($\alpha = 0$) high PM indices are encountered when the condition $\cos(\varphi + \delta/2) < c \sin(\varphi + \delta/2)$ occurs.

7) For $0 \leq \alpha \leq 6°$, $c = 0.126$ (18 db attenuation), D = 33 db, the peak carrier loop tracking error is less than $\pm 0.045 + 1.66\theta$. Substituting the maximum dynamic tracking error of $0.7°(1.22 \times 10^2$ radians) for θ, the peak error is less than 6.5×10^{-2} radians. The values of the parameters used are representative values obtained from the Dalmo-Victor reports.

8) The phase noise will not provide any serious interference with the PRN code, considering the fact that the power level of the phase noise produced by the antenna tracking system is considerably below those of the voice and telemetry subcarriers (the voice and telemetry subcarriers fall within the PRN spectrum and have modulation indices which lie between 0.76 and 1.85 while it was pointed out above that the peak phase error does not exceed 0.065 radians).

9) For the square wave IPM produced by the antenna tracking system near boresight, it is shown that the magnitude of the peak range-rate error is

$$|\dot{r}_e| \leq \frac{5.26 \times 10^3}{N} \left[1 + \frac{|\dot{r}_i|}{2.34 \times 10^5} \right] \text{ ft/sec}$$

N is the number of biased doppler cycles counted and $\dot{r}_i$ is the indicated range-rate in ft/sec. Using the extreme value of $\dot{r}_i$ for which the doppler counter is designed

$$|\dot{r}_e| \leqq \begin{cases} 6.2 \times 10^{-2} \text{ ft/sec for } 0.1 \text{ second readout interval} \\ 6.2 \times 10^{-3} \text{ ft/sec for } 1.0 \text{ second readout interval} \end{cases}$$

In the non-destructive mode, range-rate error is negligible. Hence, it is concluded that the antenna tracking system will have a negligible effect on the determination of range-rate.

Since the wide beam null depths indicated in the Dalmo-Victor reports are greater than those for the narrow beam, it is concluded that the antenna tracking system will have negligible effects on the PRN code and range-rate determination after acquisition in both the wide and narrow beam modes. The other communication services are on sub-carriers which are sufficiently far removed in the spectrum to be un-affected by the antenna tracking system. It should be pointed out that these conclusions are based upon parametric information obtained from the published Dalmo-Victor reports and a large variation from the values of the various parameters used here may necessitate a re-evaluation of these conclusions. Specifically, a null depth of 20 db rather than the 33 db used here can increase the peak-to-peak incidental phase modulation near boresight by a factor of 4 or 5. Such an increase would require a more detailed analysis than has been performed here to evaluate the deleterious effects of the antenna tracking system on communications after antenna boresight acquisition.

10) During acquisition, there is some question regarding whether or not the transponder carrier tracking loop will lock onto one of the sidebands produced by IPM. These sidebands are 100 cps apart. For the Apollo parameters, the loop 3 db bandwidth is 910 cps. With a bandwidth as wide as that indicated, it is probable that the carrier tracking loop will not lock on a sideband during acquisition. If there is serious doubt about the carrier tracking loop successfully locking to the carrier during acquisition, the possibility of locking to a sideband can be completely eliminated by temporarily suspending lobing during

acquisition until the carrier loop has locked to the uplink carrier. In the widebeam mode, there is sufficient margin to achieve carrier lock off boresight for ranges greater than 2000 nautical miles; this must be true or the antenna tracking system will not operate. Since there is no error signal (other than noise) provided for the antenna tracking system until the carrier loop has locked, there seems to be little reason for lobing until the carrier loop is in lock. It should be possible to implement the termination of lobing during carrier acquisition automatically by a system which monitors the AGC bus voltage.

11) The overall effect of the antenna tracking system on acquisition appears to be that of adding the spacecraft antenna slewing time to previous estimates of acquisition. Newman* estimates that 8.0 seconds after spacecraft illumination, two-way RF lock will have been achieved and 9.0 seconds after S/C illumination all demodulators will be locked. However, in arriving at his acquisition time estimates, Newman assumes that the spacecraft antenna is properly oriented, which will not, in general, be true with utilization of the RF antenna tracking system. Two-way RF lock is achieved in two steps: first, the spacecraft transponder is locked, then the ground receiver is locked. The spacecraft antenna does not start its motion toward the line of sight to the earth station until the spacecraft transponder is locked. If the spacecraft antenna has completed its slewing operation by the time the ground receiver is locked, there will be no increase in acquisition time. If the S/C antenna has not settled by the time the ground receiver is locked, there may be an increase in the amount of time for all demodulators to lock due to a temporary S/C antenna pointing loss. Hence, the worst case increase in acquisition time (in keeping with Newman's worst case estimates) is equal to the spacecraft antenna slewing time.

7.4 GENERAL

Further investigation should be made on the effects of elliptical polarization with existing axial ratios.

APPENDIX A
DERIVATION OF AM AND PM NEAR BORESIGHT

From Equations (1), (2), and (8) of the text, Section 5

$$E_R = \sqrt{1 + C^2} \left[E_1 e^{i\tan^{-1}C} + E_2 C^{-i\tan^{-1}C} \right]$$

$$= \sqrt{1 + C^2}\; e^{i\frac{\delta}{2}} \left[A(\theta - \alpha) e^{-i(\varphi + \frac{\delta}{2} - \tan^{-1}C)} + KA(\theta + \alpha) e^{-i(\varphi + \frac{\delta}{2} - \tan^{-1}C)} \right]$$

Expanding $\left| E_1 \right|$ and $\left| E_2 \right|$ in Taylor's series,

$$\begin{aligned} A(\theta - \alpha) &= A(-\alpha) + \theta A'(-\alpha) + \ldots \\ &= A(\alpha) - \theta A'(\alpha) + \ldots \\ A(\theta + \alpha) &= A(\alpha) + \theta A'(\alpha) + \ldots \end{aligned}$$

After substitution of the series and a little manipulation,

$$E_R = \sqrt{1 + C^2}\; e^{i\frac{\delta}{2}} (K + 1) A(\alpha) \cos\left(\varphi + \frac{\delta}{2} - \tan^{-1}C\right) \left[1 + \frac{K-1}{K+1} \frac{A'(\alpha)}{A(\alpha)} \theta + \right.$$

$$\left. + i\left\{ \frac{K-1}{K+1} + \theta \frac{A'(\alpha)}{A(\alpha)} \right\} \tan\left(\varphi + \frac{\delta}{2} - \tan^{-1}C\right) + \ldots \right]$$

Now,

$$\tan\left(\varphi + \frac{\delta}{2} - \tan^{-1}C\right) = \frac{\tan\left(\varphi + \frac{\delta}{2}\right) - C}{1 + C \tan\left(\varphi + \frac{\delta}{2}\right)} \cong 2\pi \frac{S}{\lambda} \theta + \frac{\delta}{2} - C$$

if $\delta/2 \ll 1$ radian.

After some more manipulation,

$$E_R \cong \sqrt{1+C^2}\ e^{i\frac{\delta}{2}}\ (K+1)\ A(\alpha) \cos\left(\varphi + \frac{\delta}{2} - \tan^{-1}C\right)\left[1 + \frac{K-1}{K+1}\ \frac{A'(\alpha)}{A(\alpha)}\ \theta\right] e^{i\psi_R}$$

where

$$\psi_R \cong \frac{K-1}{K+1}\left(\frac{\delta}{2} - C\right) + \left[\frac{K-1}{K+1}\ 2\pi\frac{S}{\lambda} + \left(\frac{\delta}{2} - C\right)\left\{1 + \left(\frac{K-1}{K+1}\right)^2\right\}\frac{A'(\alpha)}{A(\alpha)}\right]\theta$$

These approximations require that the first term of ψ_R be small compared to one radian.

Similarly,

$$E_L \cong \sqrt{1+C^2}\ e^{i\frac{\delta}{2}}\ (K+1)\ A(\alpha) \cos\left(\varphi + \frac{\delta}{2} + \tan^{-1}C\right)\left[1 + \frac{K-1}{K+1}\ \frac{A'(\alpha)}{A(\alpha)}\ \theta\right] e^{i\psi_L}$$

where

$$\psi_L \cong \frac{K-1}{K+1}\left(\frac{\delta}{2} + C\right) + \left[\frac{K-1}{K+1}\ 2\pi\frac{S}{\lambda} + \left(\frac{\delta}{2} + C\right)\left\{1 + \left(\frac{K-1}{K+1}\right)^2\right\}\frac{A'(\alpha)}{A(\alpha)}\right]\theta$$

$$AM = \frac{|E_R| - |E_L|}{|E_R| + |E_L|} = \frac{\cos\left(\varphi + \frac{\delta}{2} - \tan^{-1}C\right) - \cos\left(\varphi + \frac{\delta}{2} + \tan^{-1}C\right)}{\cos\left(\varphi + \frac{\delta}{2} - \tan^{-1}C\right) + \cos\left(\varphi + \frac{\delta}{2} + \tan^{-1}C\right)}$$

$$= C \tan\left(\varphi + \frac{\delta}{2}\right)$$

$$\cong 2\pi\frac{S}{\lambda}\ C(\theta + \theta_S)$$

where

$$\theta_S = \frac{\delta}{4\pi\frac{S}{\lambda}}$$

$$= \text{the amount by which the electrical boresight is shifted from the mechanical boresight}$$

$$\text{PM (peak-to-peak)} \quad = \quad \text{Arg } E_R - \text{Arg } E_L = \psi_R - \psi_L$$

$$= \quad -2C \frac{K-1}{K+1} - 2C \left\{ 1 + \left(\frac{K-1}{K+1} \right)^2 \right\} \frac{A'(\alpha)}{A(\alpha)} \; \theta$$

$$= \quad \pm 2 \left(10^{-\frac{D}{20}} \right) + \left[1 + \frac{10^{-\frac{D}{10}}}{C^2} \right] \left[-2 \frac{A'(\alpha)}{A(\alpha)} \right] \theta$$

APPENDIX B
ESTIMATION OF THE RANGE-RATE ERROR PRODUCED BY
THE ANTENNA TRACKING SYSTEM NEAR BORESIGHT

Let the carrier transmitted by the ground station be

$$v_T(t) = E_T \sin \omega_c t$$

and let the received (transponded) carrier be

$$v_R(t) = E_R \sin [\omega_c(t - \tau) + \rho \theta_e (t - \lambda)]$$

where $\theta_e (t - \lambda)$ is the transponder carrier tracking error produced by the antenna tracking system, and $\rho = 240/221$. The expression for $v_R(t)$ assumes that the ground receiver tracks $\theta_e(t)$, which results in a worst case analysis.

After biasing the received signal with a 1 mc standard, the received and transmitted signals are mixed to yield

$$v_M(t) = E_M \cos [\omega_c \tau + \omega_B t - \rho \theta_e (t - \lambda)] = E_M \cos \psi(t),$$

$$\omega_B = 2 \pi f_B = 2\pi (10^6)$$

Range information is contained in τ:

$$\tau = \tau(t) \cong \frac{2 r(t)}{c} , \quad r(t) = \text{range at time t}, \quad c = \text{velocity of light}$$

Range rate is determined by measuring the length of time it takes $v_M(t)$ to go through a given number of cycles. If N cycles of $v_M(t)$ are counted in a time interval of length T_c, then

$$\psi(t) - \psi (t - T_c) = 2\pi N$$

or

$$2\pi N = \frac{2\omega_c}{c}\left[r(t) - r(t - T_c)\right] + \omega_B T_c \rho \left[\theta_c(t - \lambda) - \theta_e(t - T_c - \lambda)\right]$$

Multiplying both sides by $c/2\omega_c T_c$ and rearranging

$$\underbrace{\frac{2\pi c(N - f_B T_c)}{2\omega_c T_c}}_{\substack{\text{indicated} \\ \text{range rate}}} = \underbrace{\frac{r(t) - r(t - T_c)}{T_c}}_{\text{true range-rate}} - \underbrace{\frac{c\rho}{2\omega_c T_c}\left[\theta_e(t - \lambda) - \theta_e(t - T_c - \lambda)\right]}_{\text{range-rate error}}$$

If we let

$$\dot{r}_i = \text{indicated range-rate}$$

$$= \frac{2\pi c}{2\omega_c T_c}(N - f_B T_c)$$

then solving for T_c

$$T_c = \frac{\dfrac{2\pi c N}{2\omega_c}}{\dot{r}_i + \dfrac{c\omega_B}{2\omega_c}}$$

and substituting in the expression for range-rate error, we have

$$\dot{r}_e = \text{range-rate error}$$

$$= -\frac{\rho\left[\theta_e(t - \lambda) - \theta_e(t - T_c - \lambda)\right]\dfrac{c\omega_B}{2\omega_c}}{2\pi N}\left[1 + \dfrac{\dot{r}_i}{\dfrac{c\omega_B}{2\omega_c}}\right]$$

Using the expression for $\theta_e(t)$ on boresight derived in the text, equation (12), an upper bound on the magnitude of the range-rate error can be established

$$\left| \dot{r}_e \right| < \frac{\rho \left| \theta_e(t - \lambda) - \theta_e(t - T_c - \lambda) \right|}{2\pi N} (2.34 \times 10^5) \left[1 + \frac{\left| \dot{r}_i \right|}{2.34 \times 10^5} \right] \text{ ft/sec}$$

where

$$\frac{c\,\omega_B}{2\,\omega_c} \cong 2.34 \times 10^5 \text{ ft/sec}$$

has been substituted.

From the analysis in the text

$$\frac{\left| \theta_e(t - \lambda) - \theta_e(t - T_c - \lambda) \right|}{2\pi} < \frac{2(6.5 \times 10^{-2})}{2\pi} \cong 2.07 \times 10^{-2}$$

The doppler counter is designed for $\pm$ 180 kc doppler biased about a 1 mc standard frequency, or an indicated range-rate of approximately $\pm$ 42,100 ft/sec. Provision is made for readout at nominal intervals of 0.1 second and 1.0 second and for continuous, nondestructive accumulation of range-rate. In the nondestructive mode, the range-rate error is negligible, since T_c becomes very large and the variation of $\theta_e(t)$ is bounded. The hardware details of the doppler counter are unknown, but it will be assumed that $N = 10^5$ for 0.1 second interval readout and $N = 10^6$ for 1.0 second readout (see the expression for T_c with $\dot{r}_i = 0$).

Using the maximum value of $\left| \dot{r}_i \right|$

$$\left| \dot{r}_e \right| < \frac{\rho (2.07 \times 10^{-2})}{N} (2.34 \times 10^5) \, [1 + 0.18] \text{ ft/sec}$$

or

$$\left| \dot{r}_e \right| < \begin{cases} 6.2 \times 10^{-2} \text{ ft/sec} & \text{for } N = 10^5 \text{ (0.1 sec readout interval)} \\ \\ 6.2 \times 10^{-3} \text{ ft/sec} & \text{for } N = 10^6 \text{ (1.0 sec readout interval)} \end{cases}$$

APPENDIX C
THE ON-LINE COMPUTING CENTER

The On-Line Computer provides the engineers and scientists at
TRW Systems with a unique facility for conducting computer-aided
research. Unlike the larger and faster 7094 computers, the On-Line
Computer can be used directly by the researcher. It was designed
specifically to make direct access to a computer easy and convenient
for the users. For this purpose the On-Line Computer has four
simultaneously operating consoles, each consisting of two keyboards
and a display storage tube. By pressing keys on the keyboards the
users initiate programs with the central processing unit which perform
useful operations. The arithmetic operations available are operations on
lists of numbers rather than on single numbers. The display storage
tube can be used to obtain graphical displays of the results of these
arithmetic operations, to label the graphs, and to print numerical values.
The symbols which can be used in these displays include not only the
letters of the alphabet and the digits 0 through 9, but also special symbols
created by the user. All displays are brought about by pressing appro-
priate keys on the keyboards. Sitting at the console the user can program
the On-Line Computer to perform any composite operation (corresponding
to pressing any sequence of keys) and can assign this console program
to a single key. One such console program can initiate other console
programs which in turn can initiate others to any degree of complexity
desired. In this way the user can develop a sophisiticated capability
for solving problems in his area of interest.

The On-Line Computer was developed by TRW for use by its tech-
nical staff. It has been widely recognized as a significant contribution
to the search for ways to facilitate communication between men and
computers.

TRW INC.

7 March 1966

National Aeronautics and Space Administration
Manned Spacecraft Center
Houston, Texas   77058

Attention: Mr. H. R. Rosenberg
               Information Systems–Systems Analysis––ISD
               Building 416, Room 116

Subject: Corrections for ASPO–18 Final Report,
               "LEM and CSM USB System RF Tracking Study"

Gentlemen:

The following errors appeared in the final report dated January, 1966:

Page 2 – Acquisition ranges were based on the angle where PM becomes excessive. The system will tolerate high PM; therefore, the acquisition ranges increase to the point where the AM reverses sign which corresponds to the region between nulls on the antenna sum patterns. There are:

	Acquisition Range
CSM wide	$\pm 70°$
CSM narrow	$\pm 5°$
LEM	$\pm 16°$

Page 4 – The horizontal scales of the lower three diagrams under Phase Comparason should be increased by a factor of two.

Page 7 – The second equation should read:

$$\frac{E_{\Delta_n}}{E_{\Sigma_\rho}} = \frac{A_1 - A_2}{A_1 + A_2}$$

Page 9 – The first equation should read:

$$\theta_s = \cot \alpha \, \frac{1 - A_1/A_2}{1 + A_1/A_2}$$

TRW SYSTEMS · HOUSTON OPERATIONS

SPACE PARK DRIVE · HOUSTON · TEXAS 77058 · AC 713-591-3133

Page 21 - Title for both figures should read-----------------------and 23 db Null.

Page A-1, line 3:

$$+KA \; (\theta + \alpha)e^{-i\left(\varphi + \frac{\delta}{2} - \tan^{-1}C\right)}$$

Should read: $+KA \; (\theta + \alpha)e^{+i\left(\varphi + \frac{\delta}{2} - \tan^{-1}C\right)}$

Page B-2: In the center of the page, the expression for indicated range-rate:

$$\dot{r}_i = \frac{2\pi c}{2\omega_c T_c} \; (N - f_B T_c)$$

Should read: $\dot{r}_i = \frac{2\pi c}{2\omega_c T_c} \; (N - f_B T_c)$

TRW SYSTEMS

John DeVillier, Manager
Apollo Communications Project Office
Apollo Spacecraft Systems Analysis Program

TCL:JD:ns

cc: Mr. M. E. Dell, PP7
     Mr. E. B. Hamblett, Jr., PS
     Mr. O. E. Maynard, PS (2)
     Apollo Document Control (2)
     Contracting Officer, Flight Support Section (2)
     Management Services Division (2)
     Technology Utilization Officer, BF34